Identification of a responsible factor for cell fate determination in early development of *D. discoideum*

細胞性粘菌における早期の分化運命決定を担う要因の解明

Ph.D. Thesis
Haruka Hiraoka

Osaka University
Graduate School of Frontier Biosciences
2020 March 25

1. Abstract

Multicellular organisms, including humans, consist of various differentiated cells to have each role. Understanding the regulatory mechanisms that determine and induce the fate of each cell is a fundamental issue in biology and medicine. The cellular slime mold *Dictyostelium discoideum* is a good model organism for studying differentiation; it proliferates as single cells in nutrient-rich conditions, which aggregate into a multicellular fruiting body upon starvation, subsequently differentiating into stalk cells or spore cells. The fate of these cells can be predicted in the vegetative phase: cells expressing higher and lower levels of *omt12* gene differentiate into stalk cells and spore cells, respectively. However, *omt12* is merely a marker gene and changes in its expression do not influence the cell fates; determinant factors remain unknown. In this study, I aimed to identify the determinant factor by characterizing the stalk-destined and spore-destined cells that were sorted based on *omt12* expression. Luciferase assay demonstrated that cellular ATP concentrations are higher in the stalk-destined than in the spore-destined cells. Live-cell observation during development using an ATP sensor probe revealed that vegetative cells with higher ATP levels differentiated into stalk cells later. Furthermore, reducing the ATP levels in the stalk-destined cells by treatment with an inhibitor of ATP production changed their cell fates into spore cells. These results suggest that cellular ATP level is one of the intrinsic factors affecting the cell fate determination in *D. discoideum* differentiation. Here, I also discussed about the relationship between cellular ATP levels and other cell fate determinants in *D. discoideum*, suggesting the possibility that there is a common regulatory mechanism among those determinant factors.

Table of contents

2. Introduction

2-1. Factors to determine the cell fate of differentiation in multicellular organism

Multicellular organisms, including humans, consist of various differentiated cells having an each role. For their proper functions, differentiation process must be regulated spatial and temporal; otherwise the errors occurred during developmental process can induce the fatal defection to organisms. Therefore, understanding the regulatory mechanisms that determine and induce the fate of each cell is a fundamental issue in the fields of biology and medicine (Castanon and González-Gaitán, 2011; Chagastelles and Nardi, 2011; Alvarado and Yamanaka, 2014; Avior et al., 2016; Zakrzewski et al., 2019). In the process of cell differentiation, following two factors act as keys for regulating and inducing differentiation: the environmental (exogenous) factors and the intrinsic factors to cause the cellular heterogeneity. Recent improvement of observation technology showed that various type of heterogeneity exist even in genetically identical cell population .

As one of the cellular heterogeneities relating to differentiation, difference of metabolic activity is known. Supporting this notion, it has been reported that glycolysis pathway is dominant over oxidative phosphorylation (reaction in mitochondria) as a means to generate energy in actively proliferating cells such as cancer cells and stem cells (Simsek et al., 2010; Koppenol et al., 2011; Ito and Suda, 2014), whereas oxidative phosphorylation become dominant toward the differentiation in human cells (Berger et al., 2016; Schell et al., 2017). The shift of metabolic pathways using preferentially is known to be important for the switch to differentiation phase from growth phase. Moreover, the activity of the mitochondrion, an organelle important for metabolism, has been reported to be crucial for the differentiation of human cells (Buck et al., 2016; Khacho et al., 2016). Those increasing evidences showed the relationship between metabolic activity and differentiation. However, the critical factors that determine cell fate of differentiation remain unknown.

2-2. *Dictyostelium discoideum* as a model organism for studying differentiation

The slime mold *Dictyostelium discoideum* is a good model organism for studying the relationship between cellular heterogeneity and differentiation. They proliferate as single amoeboid cells in nutrient-rich conditions, but aggregate and transfer into multicellular phase in response to starvation (Fig.1) (Maeda et al., 1997). At the end of development, they produce a fruiting body composed of two types of differentiated cells, i.e., stalk cells and spore cells (Fig.1). The developmental process of *D. discoideum* is initiated following the aggregation by the chemotaxis toward the cAMP (Konijn et al., 1969a; Koniijn et al., 1969b): *D. discoideum* cells have the nature to move up the gradient of cAMP (Fig.2). Therefore, cAMP sensing and directional migration is necessary for the proceeding of their differentiation process. In fact, some mutant cells with defects on this migration process show the delayed development: e.g., *gip1*- or *pten*- null mutants. (Kamimura et al., 2016; Iijima and Devreotes, 2002). Migrating cells aggregate and form multicellular body called “mound”. Cells that enter the mound phase begin to differentiate into stalk or spore progenitor cells, called prestalk and prespore cells, respectively. Prestalk cells are sorted to the top side of the mound, forming the tip region, which later forms the anterior region of the migrating body (slug), whereas prespore cells constitute the posterior region of the slug. This localization pattern is shown by observation of a slug composed of cells expressing marker genes which fused with fluorescence proteins (Fig.3); *ecmA* (Morrissey et al., 1984; McRobbie et al., 1988) and *pspA* (Grant et al., 1985; Early et al., 1988) are used as marker genes which are expressed specifically in stalk cell and spore cell, respectively. In the process of fruiting body formation, prestalk cells differentiate into stalk cells, penetrating into the prespore region of the slug. Spore cells generating progenies are moved to the top of the fruiting body through the support of stalk cells (Maeda et al., 1997).

There are three advantages in *D. discoideum* as a model organism, as follows. First, their differentiation process can be easily induced by only removal of culture medium, that is starvation. Second, whole process of differentiation can be accomplished within a relatively short time compared with other organisms; a fruiting body which is the final form of those process is obtained within 24 hours (Fig.1 and Fig.4). Third, the causal relationship between intrinsic factors and cell fates of *D. discoideum* can be discussed relatively simple, thanks to they only have two cell fates.

2-3. Factors affecting the differentiation of *D. discoideum*

Several factors have been reported to affect the cell fate determination of *D. discoideum*: intracellular calcium concentration, cell cycle stage, and metabolic activity. Calcium ion is thought as a key to regulate the various events at transition point to differentiation, because intracellular calcium concentration rapidly increases in response to starvation and achieve the peak within 30 minutes from starvation (Tanaka et al., 1998). Moreover, intracellular calcium concentration varies among cells; their concentrations are higher in the anterior prestalk region of a slug than that in posterior prespore region (Maeda and Maeda, 1973; Cubbit et al., 1995). Calcium ion is also focused as a factor to associate the differentiation and cell cycle stage, as following described. The position on cell cycle to transfer into differentiation from growth phase is called as GDT point (meaning the Growth/Differentiation Transition point) in *D. dictyostelium*; GDT point exists at G2 phase (Fig.5). Previous studies have claimed that cell fate of differentiation is determined by the distance from GDT point on cell cycle when starved (Ohmori and Maeda, 1987; Maeda et al., 1989). That is, cells before entering M phase differentiate into stalk cells later, and cells at mid G2 phase into spore cells (Fig.5). Interestingly, intracellular calcium concentrations are relatively higher in cells at S phase or early G2 phase and such cells

have stalk tendency, whereas cells at mid to late G2 phase have relatively lower calcium concentrations and have spore tendency (Azhar et al., 2001). Intracellular calcium concentration and cell cycle stage of each cell might regulate the differentiation tendency with common mechanism. Similar common points are also found between cell cycle stage and metabolic activity. Several genes expressed at GDT point have been found in previous studies (Maeda, 2005; Maeda, 2011) and they include the genes encoded by mitochondrial DNA; expressions of those mitochondrial genes are required in transition to differentiation (Inazu et al.,1999; Maeda, 2005). Other metabolism-related factors affecting the differentiation are also known; for example, the changes in mitochondrial respiratory activity and those in mitochondrial morphology affect cell differentiation (Leach et al., 1973; Matsuyama and Maeda, 1995; Chida et al., 2004; Kimura et al., 2010). Like humans and other higher eukaryotes, it has also been reported that mitochondrial activity is crucial when switching from growth to differentiation in cellular slime mold. Furthermore, previous studies have reported that differentiation tendency is affected by the presence or absence of glucose, an essential molecule in the glycolysis pathway, in the culture medium (Leach et al., 1973; Tasaka and Takeuchi, 1981; Thompson and Kay, 2000; Chattwood and Thompson, 2011). Many studies have shown the relationship between metabolism and differentiation of *D. discoideum*.

2-4. Prediction of cell fates at the vegetative phase before differentiation

As described in previous section, complicated crosstalk between several factors affecting the cell fate determination is known in *D. discoideum*. Some of these factors, like the cell cycle stage when starved and the glucose concentration in culture medium, reflect the condition of vegetative cells. These studies have provided us an idea that cell fates might be determined at the vegetative phase, in contrary to the fact that a stalk and a spore

marker gene does not express until slug phase (middle and bottom panels of Fig.3). This contrary has been discussed for long time.

However, recent study put an end to the discussion by showing that cell fates of *D. discoideum* can be predetermined at the vegetative phase before multicellular formation (Kuwana et al., 2016). The cell fates are distinguished by their expression levels of the *omt12* gene at the vegetative phase; vegetative cells expressing high levels of *omt12* (termed as pstVA in (Kuwana et al., 2016)) are destined to differentiate into stalk cells (designated as "stalk-destined" cells, hereafter), whereas vegetative cells expressing low levels of *omt12* are destined to differentiate into spore cells (designated as "spore-destined" cells, hereafter). At first, *omt12* was identified as one of the genes expressed higher in anterior prestalk region than in posterior prespore region (SSK861 in Maeda et al., 2003). The gene product is o-methyl transferase (OMT) family protein modifying the resorcinol ring to synthesize a variant of 4-methyl-5-pentylbenzene-1, 3-diol (MPBD) (Ghosh et al., 2008). MPBD has been reported to be involved in various events in development: e.g., cAMP signaling in early development, prestalk/prespore pattern formation, and spore differentiation (Saito et al., 2006; Narita et al., 2011; Sato et al., 2013; Narita et al., 2014). For these reasons, *omt12* was especially focused as a candidate involved in differentiation and further investigated in Kuwana et al. (2016).

Identifying *omt12* as a marker gene allows us to distinguish between stalk-destined and spore-destined cell at the vegetative phase before differentiation. However, *omt12* is merely a marker gene and changes in its expression levels did not influence the differentiation (Kuwana et al., 2016). Determinant factors remain unknown.

2-5. The analyses performed in this study

In this study, I aimed to identify the actual factors to determine cell fates by applying the advantage that cell fates can be predicted at the vegetative phase. Specifically, I separately collected the stalk-destined and spore-destined cells according to *omt12* gene expression levels and characterized the sorted cells.

I first performed RNA sequencing (RNA-seq) analysis to examine the differences in gene expression levels between the stalk-destined and spore-destined cells. The results of RNA-seq analysis suggested the activation of metabolic activity in the stalk-destined cells. To prove this, I next measured the cellular concentration of ATP, a product of metabolism, at the vegetative phase by both luciferase assay and microscopy. For microscopic observation, I developed new ATP sensor probes which optimized for *Dictyostelium*. ATP levels of the stalk-destined and spore-destined cells were also monitored during development. As these experiments suggested the influence of ATP to differentiation, I investigated the mechanism by ATP affect the developmental process, by observing the fates of cells treated by inhibitors of ATP production and that of sorted cells according to ATP levels.

Finally, I discussed the relationship between the influence of ATP found in this study and other determinant factors which have been reported previously: intracellular calcium concentration, cell cycle stage, and their crosstalk.

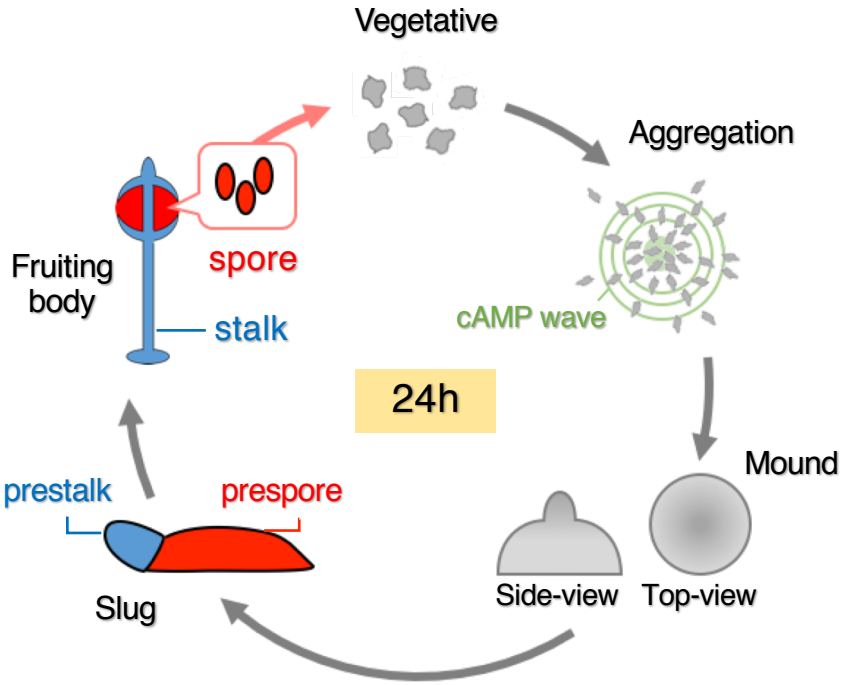

Fig.1 Schematic image of development of *Dictyostelium discoideum*

Schematic illustration of the developmental process of *Dictyostelium discoideum*. They transfer to the developmental process in response to starvation. A slug consists of prestalk cells at the anterior region (blue) and prespore cells at the posterior region (red). Prestalk cells differentiate into stalk, and prespore cells differentiate into spore cells in a fruiting body. Next generation amoeba cells are germinated from spore cells. Fruiting body is usually formed within 24 hours.

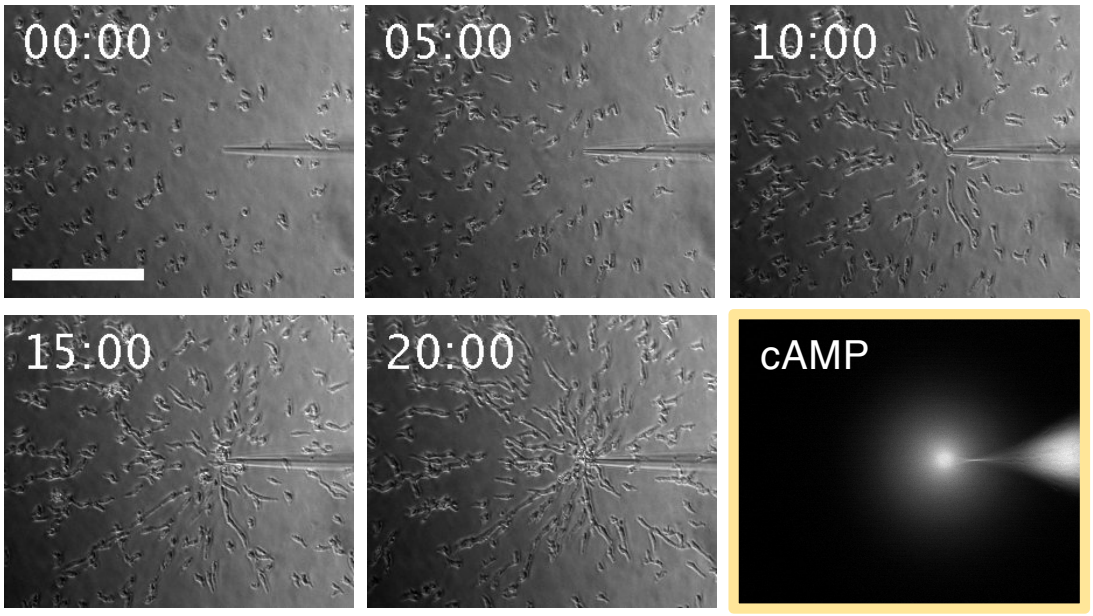

Fig.2　Chemotaxis to cAMP

Images showing the chemotaxis of wild-type Ax2 cells to 1μM cAMP solution provided from the needle on the right in each image. Images were acquired every 5 seconds by CM using a 10× objective lens. The number in each image indicates time in minutes: seconds. An image on right-bottom represents the diffusion pattern of cAMP; cAMP solution with fluorescent dye, ATTO532, was used here for the visualization of cAMP. Scale bar, 50 μm.

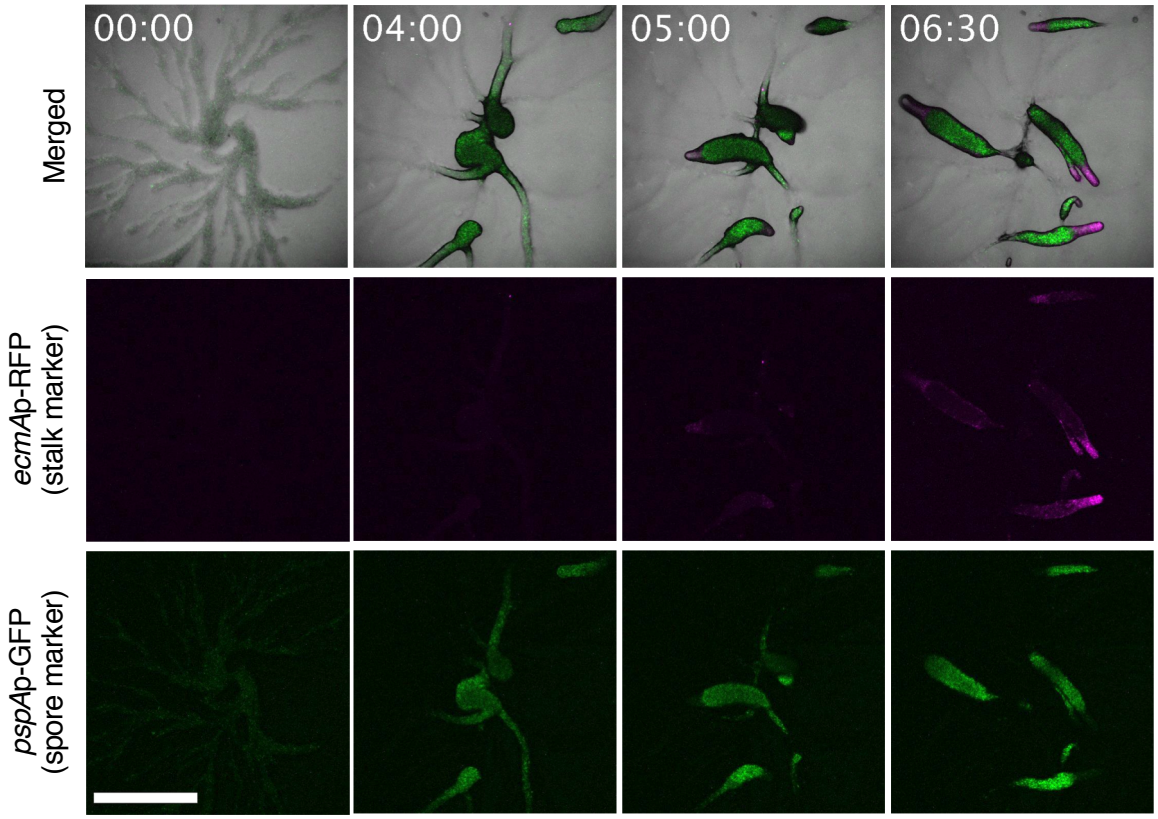

Fig.3 Expression of stalk marker and spore marker genes at the slug phase

Developmental process of cells expressing both *ecmA*p-RFP and *pspA*p-GFP; *ecmA* and *pspA* is a marker gene expressing specifically in stalk and spore cell, respectively. Merged images of bright-field and fluorescence images (top), RFP fluorescence images (middle, stalk marker) and GFP fluorescence images (bottom, spore marker) are shown. Prestalk cells expressing *ecmA*p-RFP and prespore cells expressing *pspA*p-GFP localized at anterior region and posterior region in a slug, respectively (see also the schematic image in Fig.1). Z-stack images were acquired every 10 minutes by FV1000 using a 20× objective lens and projected with the maximum intensity using Fiji. The number in each image indicates time in hours: minutes. Scale bar, 500 μm.

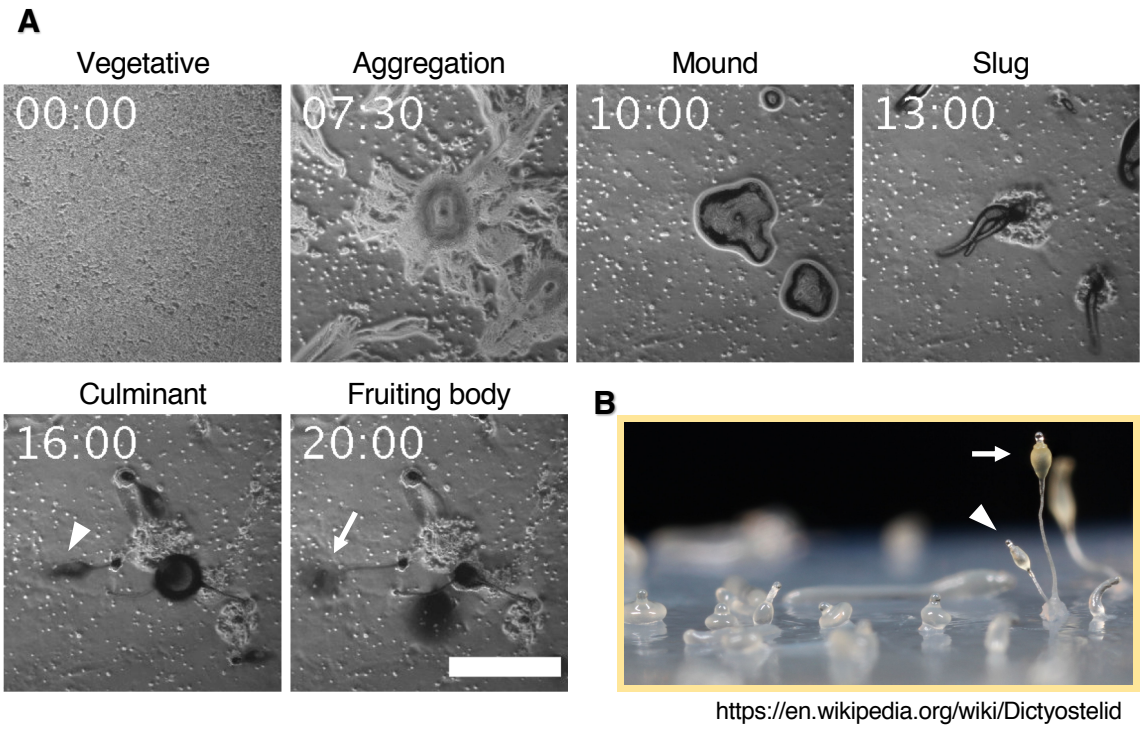

Fig.4 Progress time of developmental process of *D. discoideum*

(A) Representative progress time of developmental process of *D. discoideum*. Images were acquired every 10 minutes by CM using a 10× objective lens. The number in each image indicates time in hours: minutes. White arrowhead in "16:00" and arrow in "20:00" indicate the fruiting body under formation; they are corresponding to the same marks shown in (B). Fruiting bodies are out of focus due to their 3D structures. Scale bar, 500 μm.

(B) Side-view images showing the whole developmental process of *D. discoideum*; it is referred from "https://en.wikipedia.org/wiki/Dictyostelid". White arrowhead and arrow indicate the side-view images of structures shown in "16:00" and "20:00" of (A), respectively.

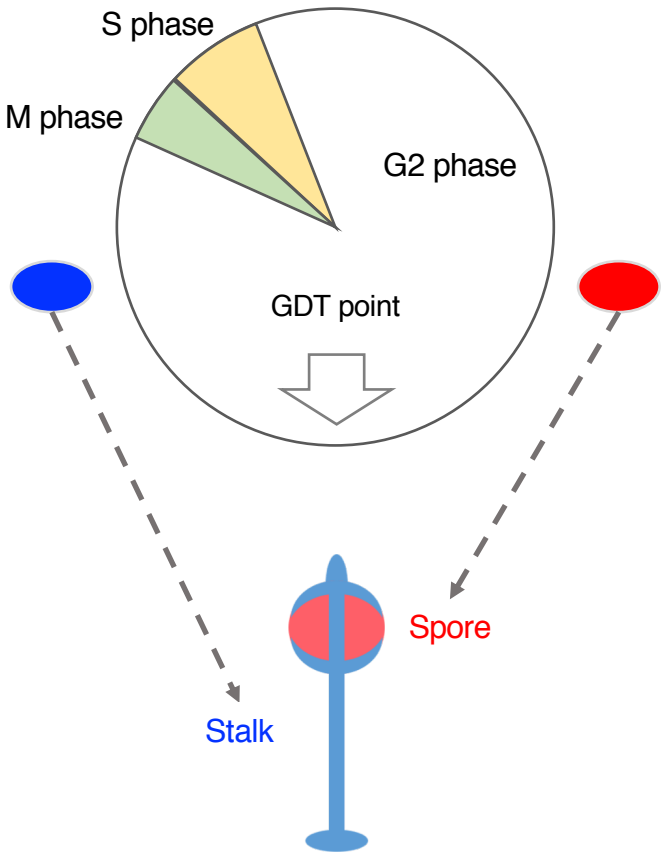

Fig.5 The relationship between cell fate and cell cycle stage

Schematic images showing the relationship between the cell fate and the cell cycle stage described in previous studies (Maeda, 2005; Maeda, 2011). White arrow indicates the GDT point (the transition point to differentiation from growth) existing at G2 phase. Cells positioned after GDT point differentiate into stalk cells, whereas cells positioned before GDT point differentiate into spore cells.

3. Materials and Methods

3-1. Plasmid constructs

The pDM vector series (Veltman et al., 2009) were used as backbone vectors for generating new constructs. pDM358-*omt12*p-mCherry construct was generated from pDM304-*omt12*p-mCherry construct (a kind gift from Drs. Hashimura and Ueda, Osaka Univ.) as follows: *omt12*p-mCherry region was excised by digestion with BglII and SpeI restriction enzymes, and inserted into pDM358 vector in order to render the drug resistance to hygromycin from neomycin. Promotor sequence of *omt12*p-mCherry was amplified same as *omt12*p-GFP construct (Kuwana et al., 2016) by Dr. Hashimura. A DNA plasmid coding mRFPmars under the promoter of *act15* gene (*act15*p), one of the house keeping genes, was used as a control construct containing only fluorescence protein; *act15*p-mRFPmars sequence was inserted into pDM358 (designated as pDM358-*act15*p-mRFPmars). This construct is a kind gift from Mr. Degawa and Dr. Ueda (Osaka Univ.). To visualize the cellular ATP level of *D. discoideum*, the DNA sequences of MaLionG (Arai et al., 2018) and AT1.03NL (Imamura et al., 2009; Tsuyama et al., 2013), ATP sensor probes used in human cells, were codon-optimized for *D. discoideum*; such optimized ATP sensors were named as DicMaLionG and DicAT1.03NL, respectively. That optimization and DNA synthesis were performed by GenScript service (https://www.funakoshi.co.jp/contents/687) based on the codon usage information of *D. discoideum* (http://www.kazusa.or.jp/codon/cgi-bin/showcodon. cgi?species=44689) and their sequence information (Arai et al., 2018; for MaLionG) (Imamura et al., 2009; Tsuyama et al., 2013; for AT1.03NL). That synthesized DNA fragments were digested by BglII and SpeI restriction enzyme and inserted into pDM304 vector carrying neomycin-resistant sequence. DicMaLionR construct, where the GFP sequence of MaLionG was replaced by RFP sequence, was made by Miss Mori with the same procedures as described above.

3-2. *D. discoideum* strains

D. discoideum wild-type strain Ax2 (in-house strain) was used as a parental strain. The strain was cultured at 22°C in HL5 medium (pH 6.4-6.7) consisting of 86 mM glucose (049-31165, WAKO), 7.15 g/L yeast extract (212750, BD Biosciences), 14.3 g/L proteose peptone (212120, BD Biosciences), 3.6 mM KH_2PO_4 (169-04245, WAKO), 3.6 mM $Na_2HPO_4 \cdot 12H_2O$ (196-02835, WAKO), 453 nM folic acid (060-01802, WAKO) and 44 nM VB12 (220-00346, WAKO). 10 μg/ml Streptomycin/Penicillin (SP) solution (168-23191, WAKO) was supplemented in HL5 medium for preventing the bacteria contamination.

The neomycin-resistant *omt12*p-GFP strain was obtained as described previously (Kuwana et al., 2016). As a control against *omt12*p-GFP strain, *act15*p-mRFPmars strain (a kind gift from Mr. Degawa and Dr. Ueda, Osaka Univ.) was used. Cell strains constitutively expressing DicMaLionG or DicAT1.03NL were generated by transfecting the pDM304-DicMaLionG DNA plasmid or the pDM304-DicAT1.03NL DNA plasmid, respectively, to wild-type Ax2 strain by electroporation; 20 μg/mL neomycin (074-05963, FUJIFILM Wako Pure Chemical Corp., Osaka, Japan) was used for the selection. pDM358-*omt12*p-mCherry DNA plasmids were transfected by electroporation to DicMaLionG strain for simultaneous imaging of *omt12* expressions and ATP levels (designated as *omt12*p-mCherry/DicMaLionG), and pDM358-*act15*p-mRFPmars DNA plasmids were also transfected to DicMaLionG strain as a control (designated as *act15*p-mRFPmars/DicMaLionG); 20 μg/mL hygromycin (084-07681, FUJIFILM Wako Pure Chemical Corp.) and 20 μg/mL neomycin were used for the selection of these double-expressing strains .

Electroporation was performed using an ECM830 electroporator (BTX) in all experiments (electric conditions：500 V, 100 μs × 10 pulses, 1-s interval). Clonal cells

were selected on the basis of fluorescence intensity on a 96-well plate (1860-096, IWAKI Science Products, Shizuoka, Japan) and used for this study.

3-3. Induction of cell differentiation

First, 1% Bacto agar (214010, BD Biosciences) plates were prepared as a platform of development. Bacto agar was dissolved in milliQ and applied 1mL in 35 mm plastic dish (3000-035, IWAKI). Cultured cells were washed twice with the potassium phosphate buffer (KK2: 16.1 mM KH_2PO_4, 4.0 mM K_2HPO_4, pH 6.1) and suspended at a cell density of 4×10^7 cells/mL in same buffer for inducing the development by starvation. Then, 5-uL droplets of cell suspensions were spotted on Bacto agar plate and left still for 10 minutes for cell attachment to agar. Extra solution should be removed by tilting dishes after cell attachment for dry. Starved cells were incubated over night at 22°C to proceed the developmental process.

3-4. Flow cytometry and cell sorting

For preparations of samples for flow cytometry, fluorescent cells of interest were first suspended at a density of 5×10^6 cells/mL in HL5 medium. Then, 1 mL of the cell suspension was subjected to centrifugation to collect the cells as a pellet. The pellets were washed twice with KK2 buffer and resuspended in 0.8–1 mL of 0.3 mM EDTA in KK2 buffer to avoid cell-cell adhesion. During this process of sample preparations, cells were kept on ice. Then the cell suspension was analyzed by a FACSAria III flow cytometer (BD Biosciences, Franklin Lakes, NJ, USA).

Cell sorting according to the fluorescence intensity was performed using a sorting system of the same flow cytometer. To set the sorting gate against fluorescent cells of interest, wild-type Ax2 cells were used as negative control with no fluorescence; they

were prepared as described above. The sorting gates was set in the order of FSC-A/SSC-A, FSC-A/FSC-W, SSC-A/SSC-W, and Fluorescence-A/count. Cells with the top 5% fluorescence intensity and those with the bottom 5% fluorescence intensity were sorted and used for subsequent experiments. The sorted cells were collected in 2 mL of HL5 medium containing 30 μg/mL chloramphenicol (08027-14, Nacalai Tesque, Kyoto, Japan). This medium containing the sorting solution was replaced with fresh HL5 medium within 2 hours after sorting because sorting solution damage the sorted cells. These cells were cultured in the medium for 4–12 hours to recover from cell damage caused by the cell sorting procedure and were then used for subsequent experiments. The quality of cell sorting was evaluated by reanalyzing the fluorescence distribution of the sorted cells. For re-analysis, sorted cells were collected in 200 μL of 0.3 mM EDTA in KK2 buffer and be analyzed again by flow cytometer. The quality-checked cell fractions were used for further analysis.

3-5. RNA extraction and RT-PCR

Total RNA was extracted from the stalk-destined and spore-destined cells (high and low expressing *omt12*p-GFP, respectively; quality-checked sorted cells) using the RNeasy Plus Mini Kit (74134, QIAGEN), followed by the removal of contaminated genomic DNA using the RNase-free DNase set (79254, QIAGEN). Then, 1 μg of the extracted total RNA was reversely transferred into cDNA using M-MuLV Reverse Transcriptase (M0253S, New England BioLabs, Tokyo, Japan). RT-PCR was performed with THUNDERBIRD SYBR qPCR Mix (QPS-201, TOYOBO, Osaka, Japan) using the cDNAs as templates by Eco Real-Time PCR system (Illumina, San Diego, CA, USA). The PCR conditions were as follows: 1 cycle at 95°C for 1 minute and 40 cycles at 95°C for 15 seconds, 55°C for 15 seconds, and 72°C for 30 seconds. The DNA sequences used

as forward and reverse primer for the quantification of GFP expression were 5′-ATGTCTAAAGGAGAAGAACTTTTC-3′ (synthesized by FASMAC, Atsugi, Japan) and 5′-TAAGTTTTCCGTATGTTGCATC-3′ (synthesized by Sigma-Aldrich Inc., Tokyo, Japan), respectively.

3-6. RNA-sequencing analysis

The quality-checked cell fractions of stalk-destined and spore-destined cells were used for the RNA-sequencing (RNA-seq) analysis. Total RNAs were extracted and the quality of them were checked by the quantification of GFP expressions as described above. Comprehensive RNA-seq analyses were performed three times by the NGS service (http://ngs-service.biken.osaka-u.ac.jp/index.php/ja/pricing-and-ordering-2/) of the Genome Information Research Center (Osaka University, Suita, Japan). The differences of expression of each gene between stalk-destined and spore-destined cells were evaluated by the ratio of expressions in stalk-destined cell to those in spore-destined cell.

Measurements were performed in three biological replicates to obtain FPKM values and counts. Genes were excluded by two thresholding steps: first, genes with counts below 10 in either of the three experiments were excluded because these genes produce unreliable values for the stalk/spore ratio; second, genes with larger than 2-fold variations in the stalk/spore ratio across the three experiments were excluded to ensure reproducibility.

To analyze the differences in the gene expression levels between the stalk-destined and spore-destined cell, the genes of interest were selected based on the annotation in the *Dictyostelium* database (dictyBase; http://dictybase.org). Metabolism-related genes were selected using the words “metabolic process,” “glycolytic process,” and “TCA cycle” in the gene ontology section of the dictyBase. calcium-related genes

were selected using the phrase “upregulated in the presence of calcium” in the “gene description” section of the dictyBase. Cell cycle-related genes were selected by referring to previous studies on the relationship between cell cycle and differentiation (Maeda, 2005; Maeda, 2011).

3-7. Luciferase assay for the quantification of cellular ATP concentrations

ATP quantification was performed against cells in HL5 medium. Cells were suspended at a density of 2×10^5 cells/mL. Then, 50 μL of the cell suspension (containing 1×10^4 cells) and the same volume of CellTiter-Glo2.0 assay solution (G9242, Promega, Madison, WI, USA) were added into each well of a white 96-well plate (3912, Corning, Corning, NY, USA) and mixed vigorously by shaking for 5 minutes at room temperature (25°C). The specimens were left undisturbed on a bench for 30 minutes at room temperature to allow the reaction to occur, and then the amount of luminescence was measured for 1 second using a luminometer (GloMax, Promega, Madison, WI, USA). Various concentrations of ATP solutions were prepared from ATP powder (01072-11, Nacalai Tesque, Kyoto, Japan) for plotting a calibration curve; they were dissolved in HL5 medium as with the cells. Cellular ATP concentration was calculated from the amount of luminescence in the wells with the assumption that a cell is spherical with a diameter of 10 μm.

3-8. Fluorescence live-cell imaging

Fluorescence live-cell imaging was performed by confocal microscopy as described below. Snapshot images were acquired with FV1000 (Olympus, Tokyo, Japan) using 10× (UPlanSApo 10×/0.40 NA, Olympus), 20× (UPlanSApo 20×/0.75 NA, Olympus), 40× (UPlanSApo 40×/0.95 NA, Olympus), or 60× oil immersion (UPlanApoN 60×/1.42 NA,

Olympus) objective lens. Diode lasers and HeNe lasers were used as sources for providing 473-nm (GFP excitation) and 559-nm (RFP excitation) wavelength lights, respectively. Time-lapse images were acquired using Dragonfly200 (Andor, Tokyo, Japan) equipped with EMCCD (iXonUltra 888, Andor) cameras using 20× (Plan Apo 20×/0.75 NA, Nikon, Tokyo, Japan) or 60× oil immersion (Apo 60×/1.40 NA, Nikon) objective lenses. A solid-state laser (ILE-400, Andor) was used as the source for providing 488-nm (GFP excitation) and 561-nm (RFP excitation) wavelength lights. FRET images of DicAT1.03NL cells were acquired by LSM780 (Zeiss, Jena, Germany) using 20× (Plan-Apochromat 20×/0.8 NA, Zeiss), 40× water immersion (C-Apochromat 40×/1.20 NA, Zeiss), or 60× oil immersion (Plan-Apochromat 63×/1.40 NA, Zeiss) objective lenses. Multi Ar lasers were used for providing 458-nm (CFP excitation) wavelength light. The FRET images show the ratio intensities of YFP (ATP-bound)/CFP (ATP-free) representing the ATP levels; they were obtained using "Ratio Plus," a plugin of the Fiji software (ver. 2.0.0-rc-69/1.52p, https://fiji.sc (Schindelin et al., 2012)).

For observing the developmental process of *D. dictyostelium*, development was induced on the agar plate as described above. Then, a piece of agar plate was cut out and placed upside-down on a 35-mm glass-bottom dish (P35G-1.5-14-C, MatTek, Ashland, MA, USA) coated by 10 μL of liquid paraffin (261-17, Nacalai Tesque, Kyoto, Japan). Wet papers were placed on the lid and around the glass part of the dish, and the dish was sealed with parafilm to prevent drying during time-lapse imaging. Z-stack images (5-μm steps for 80–100 μm) were observed for acquiring the whole images of the 3D multicellular body. To observe the single cells, cells were plated on the glass-bottom dish and the dish was filled with 2 mL of KK2 buffer after cell attachment. For long-term observation, 2 mL of mineral oil was layered on the KK2 buffer to prevent drying.

3-9. Tracking the cells of interest during development

For inducing development, cells were washed twice with KK2 buffer and suspended in the same buffer as described in previous section. In order to make it easy to track fluorescently labeled cells during the developmental process, only 1–5% of labeled cells were mixed with wild-type Ax2 cells with no fluorescence. For tracking cells in early development (the vegetative phase to the mound phase), 20 μL of the mixed cell suspension at a density of 5×10^6 cells/mL (containing 1×10^5 cells) was added into each well of a 384-well glass-bottom plate (781091, Greiner Bio-One Japan, Tokyo, Japan) to limit their movements to a small area. Then, 10 μL of excess solution was removed after cell attachment, and 40 μL of 2% low-melting-point agarose (15517-022, Gibco-BRL, Cheshire, UK) in milliQ was layered on the cell suspension for flattening the 3D multicellular body. For tracking cells in late development (the mound phase to the slug phase), mixed cells were developed on the agar plate and a piece of agar was cut out and observed as described in previous sections. Cell tracking analysis against this observation was performed by the 3/4D Image Visualization and Analysis Software "Imaris" (ver.9.3.1, Bitplane AG, Abingdon, UK; https://imaris.oxinst.com).

3-10. Treatment with inhibitor drugs of ATP production

For decreasing the ATP levels of cells, 3-Bromopyruvic acid (3-BrPA; sc-260854, Santa Cruz Biotechnology, Dallas, TX, USA) or oligomycin (mixture of A, B, and C isomers; O-500, Alomone Labs, Jerusalem, Israel), inhibitors of ATP production, was added to HL5 medium at the final concentrations of 1 mM and 2.5 μM, respectively. Cells were incubated at 22°C in HL5 medium containing each inhibitor for 24 hours, washed twice with KK2 buffer or HL5 medium, and then suspended in the same buffer for subsequent experiments.

4. Results

4-1. Gene expression analysis against stalk-destined and spore-destined cells

I compared the gene expression levels of stalk-destined and spore-destined cells about all genes of *D. discoideum*. Those two cell populations were separately collected by a cell sorter according to the GFP expression of *omt12*p-GFP cells at the vegetative phase (Fig.6), and total mRNAs contained in those cells were extracted to quantify the gene expression levels; the sorting quality was confirmed by both re-analysis of sorted cells and the quantification of GFP expression levels by RT-PCR (Fig.7). Then, comprehensive RNA-sequencing (RNA-seq) analyses against such quality-checked RNA samples were performed three times; 8,191 genes out of all 12,257 genes of *D. discoideum* were detected in total. RNA-seq results showed that the expression levels were different more than 2 folds between stalk-destined and spore-destined cells in 31 genes; out of the 31 genes, 17 were higher in stalk-destined cells and 14 were higher in spore-destined cells (Fig.8 and Table.1). However, the functions of majority of such genes were unknown.

In order to identify the factors inducing the different cell fates in stalk-destined and spore-destined cells, I focused several factors which have been reported to affect the developmental process of *D. discoideum*: i.e., intracellular calcium concentration, cell cycle stage, and metabolic activity. I examined the expression levels of genes related to them. The results studying about metabolic activity will be explained from next chapter, and the consideration about other factors will be discussed later in chapter 4-9.

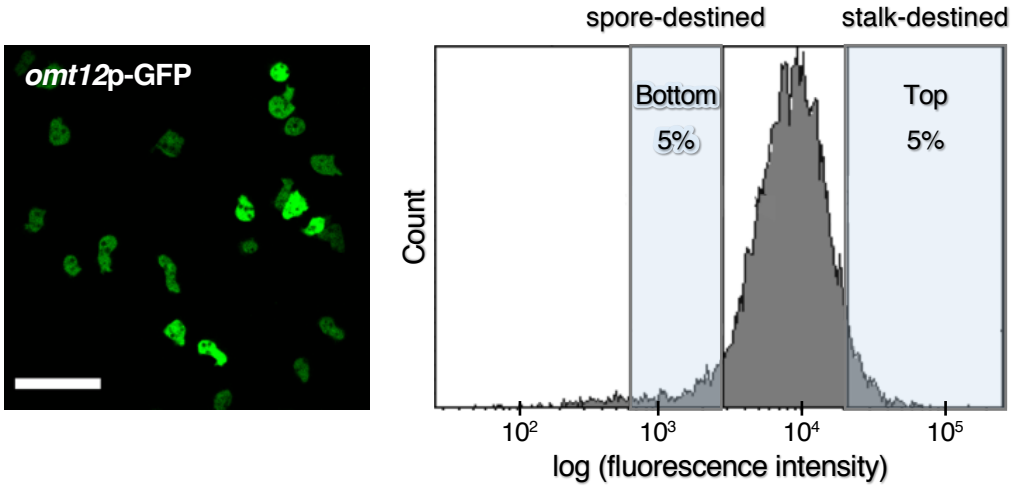

Fig.6 Sorting of the stalk-destined and spore-destined cells

A typical image of amoeba cells expressing *omt12*p-GFP used for cell sorting (left) and a typical distribution of the fluorescence intensity of *omt12*p-GFP cells measured using a flow cytometer (right). Top 5% and bottom 5% of *omt12*p-GFP-expressing cells were collected as the stalk-destined and spore-destined cells, respectively, and used for further analysis. Scale bar, 50 μm.

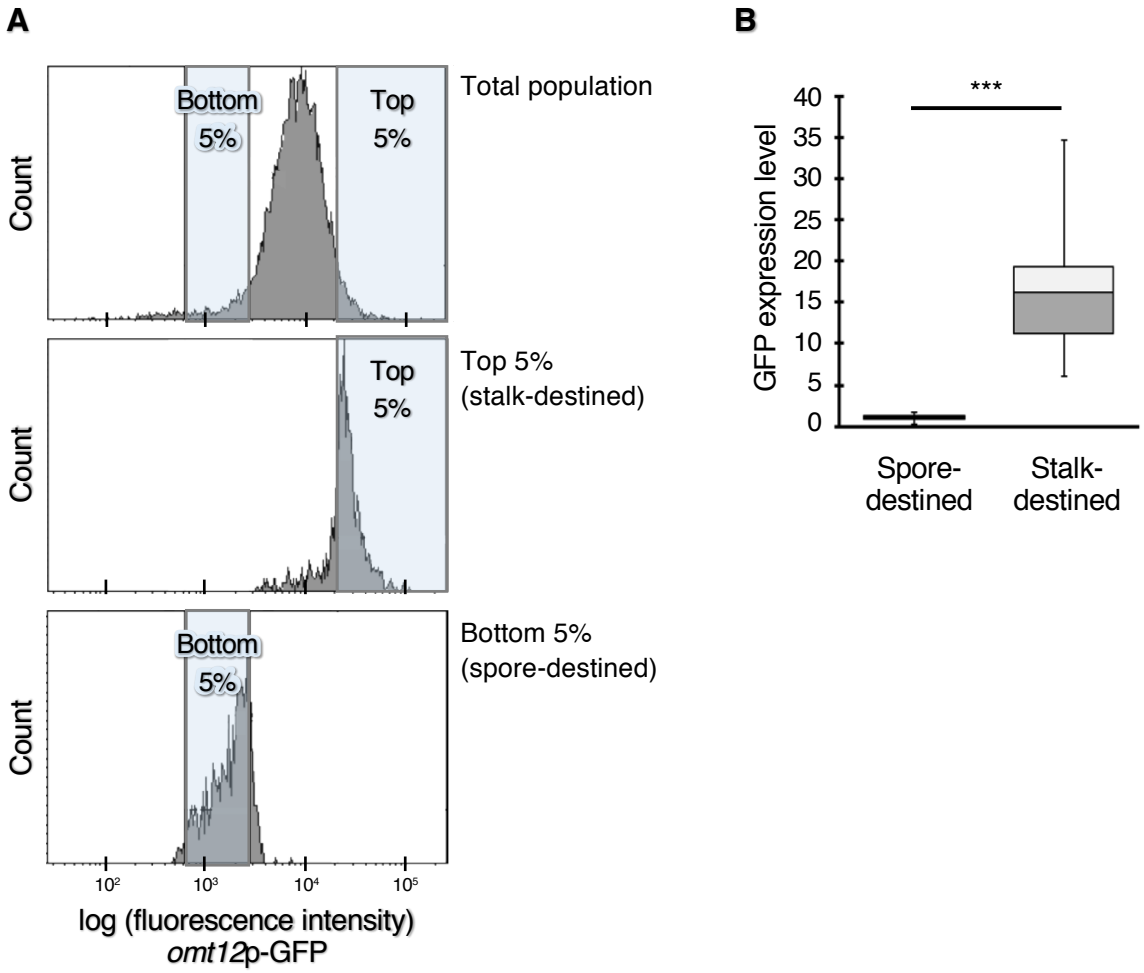

Fig.7 Quality check of cell sorting

(A) Fluorescence intensity of *omt12*p-GFP cells was measured by flow cytometry before and after sorting to quality-check the cell specimens. Typical fluorescence intensity distributions of total cell population before sorting (top panel), sorted cells of top 5% populations (stalk-destined; middle panel), and bottom 5% populations (spore-destined; bottom panel) are shown.

(B) Expression levels of *omt12*p-GFP measured by RT-PCR in the spore-destined and stalk-destined cells sorted as in (A). The average expression level in the spore-destined cells was set to 1. The number (n) of measurements; n = 29 and 28 from the left. The data is presented as box-and-whisker plots: the box indicates the median and the upper and lower quartiles; the whisker indicates the range. Data were analyzed by the unpaired two-tailed Student's t-test. ***$p < 0.001$.

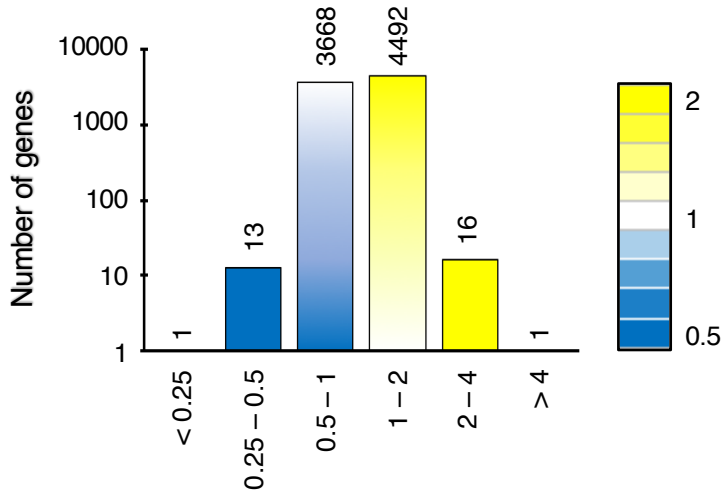

Fig.8 RNA-seq results for all genes

Analysis of RNA-seq results. The ratio of the expression of a particular gene in the stalk-destined cell to that in the spore-destined cell (stalk/spore ratio) was calculated for 8,191 genes; average values of three trials were plotted as a histogram on a semilogarithmic graph. The number at the top of each column indicates the number of genes belonging to that group. The color scale is given on the right, and the numbers on the right of the color scale are ratios.

Table.1 Genes with large differences as much as 2-fold

List of 31 genes with large differences of expression between stalk-destined and spore-destined cells: 17 genes with high expression in the stalk-destined cells (listed in upper part) and 14 genes with high expression in the spore-destined cells (listed in lower part). The "Ratio" values indicate mean of three RNA-seq measurements.

		Gene name	Protein name	Ratio
Higher in stalk-destined cells	1	DDB_G0268640	hypothetical protein DDB_G0268640	5.030
	2	DDB_G0276219	hypothetical protein DDB_G0276219	3.102
	3	DDB_G0280703	elongation factor 1b-related protein	3.006
	4	DDB_G0290545	hypothetical protein DDB_G0290545	2.749
	5	DDB_G0276731	hypothetical protein DDB_G0276731	2.739
	6	abcC10	ABC transporter C family protein	2.685
	7	DDB_G0284277	hypothetical protein DDB_G0284277	2.435
	8	abcG10	ABC transporter G family protein	2.375
	9	DDB_G0272160	hypothetical protein DDB_G0272160	2.334
	10	cinB	esterase/lipase/thioesterase domain-containing protein	2.329
	11	DDB_G0275161	hypothetical protein DDB_G0275161	2.234
	12	DDB_G0272146	hypothetical protein DDB_G0272146	2.193
	13	DDB_G0276097	hypothetical protein DDB_G0276097	2.172
	14	cbpD1	calcium-binding protein	2.112
	15	DDB_G0288507	arylamine N-acetyltransferase family protein	2.045
	16	DDB_G0290975	alpha/beta hydrolase fold-3 domain-containing protein	2.026
	17	cafA	hypothetical protein DDB_G0277827	2.001
Higher in spore-destined cells	1	DDB_G0288591	short-chain dehydrogenase/reductase family protein	0.497
	2	expl2	expansin-like protein	0.495
	3	DDB_G0271218	hypothetical protein DDB_G0271218	0.482
	4	DDB_G0280051	hypothetical protein DDB_G0280051	0.476
	5	DDB_G0267868	hypothetical protein DDB_G0267868	0.430
	6	DDB_G0280461	LISK family protein kinase	0.425
	7	DDB_G0281607	hypothetical protein DDB_G0281607	0.423
	8	cnrJ	carbohydrate-binding domain-containing protein	0.414
	9	DDB_G0269452	hypothetical protein DDB_G0269452	0.350
	10	DDB_G0287581	hypothetical protein DDB_G0287581	0.341
	11	celB	cellulase 270-11	0.317
	12	DDB_G0282715	hypothetical protein DDB_G0282715	0.313
	13	sigB	"peptidase M8, leishmanolysin family protein"	0.312
	14	DDB_G0280919	hypothetical protein DDB_G0280919	0.239

4-2. Higher metabolic activity in stalk-destined cells

A metabolism-related factor, in particular, the glucose concentration in culture medium is known as one of the factors to affect the cell fate determination in *D. discoideum*. Previous studies have reported that undifferentiated amoeboid cells cultured in a glucose-free medium differentiate into stalk cells when mixed with cells cultured in a glucose-containing medium (Leach et al., 1973; Tasaka and Takeuchi, 1981; Thompson and Kay, 2000; Chattwood and Thompson, 2011). So I examined the expression levels of 304 metabolism-related genes selected based on the annotation in *Dictyostelium* database (dictyBase, http://dictybase.org); genes annotated by "metabolic process", "glycolytic process", and "tricarboxylic acid (TCA) cycle" were selected as metabolism-related genes. Then I calculated the ratios of the expression levels in the stalk-destined cells to that in spore-destined cells for each gene. Result showed that 210 genes, corresponding to an approximately 70% of metabolism-related genes, expressed higher in stalk-destined cells than in spore-destined cells (Fig.9A). Furthermore, the group contains 6 limiting enzymes functioning in the major metabolic pathways: glycolysis and TCA cycle (Fig. 9B and Table.2). Glycolysis and TCA cycle are parts of major metabolic pathways called central metabolism, producing ATP molecules as energy resource. So these results of gene expression analysis suggested that ATP production is more activated in stalk-destined cells than in spore-destined cells.

Then, I quantified the cellular ATP concentrations of them by luciferase assay. ATP quantification was performed against stalk-destined and spore-destined cells incubated for 4-12 hours after cell sorting to reduce the cell damage caused by sorting. This incubation time was confirmed to be proper, as the ATP concentrations of cells incubated for longer than 4 hours (4, 8, 12, 24 hours) were kept constant as higher levels than that of cells just after sorting (Fig.10). Although 24-hours incubation was also proper

in the perspective of ATP level, it had a problem in the quality of sorted cells; the distribution of GFP fluorescence intensity of sorted cells started to move back to unsorted distribution 12 hours later, and in particular, the distribution of bottom 5% populations (spore-destined cells) at 24-hours-later completely changed (Fig.11). To keep the quality of the sorted cells, I set the up-limit of incubation time as 12 hours later from sorting and performed the following experiments in this rule.

Luciferase assay for ATP quantification revealed that stalk-destined cells actually had higher ATP concentrations than spore-destined cells at the vegetative phase (Fig.12). As a control, same assay was performed using *act15*p-mRFPmars cells instead of *omt12*p-GFP cells; *act15* is one of the house-keeping genes expressing constantly. Cells with the top 5% fluorescence intensity and those with bottom 5% fluorescence intensity were sorted respectively (Fig.13A), and their ATP concentrations were measured by luciferase assay. Result showed that cells in either populations had statistically same ATP levels (Fig.13B), indicating that expression of fluorescence protein itself makes no influence to cellular ATP concentrations. These results demonstrated that stalk-destined cells (highly expressing *omt12*p-GFP) had higher ATP concentrations at the vegetative phase, perhaps due to the multiplication of the slightly higher expressions of metabolism-related genes.

However, this result of ATP quantification was obtained in not-physiological condition as the used cells were sorted and eluted for luciferase assay. In order to confirm this result in physiological condition, I tried to investigate the correlation between *omt12* expressions and ATP levels by microscopy. For this purpose, I first established the ATP sensor probes working in *D. discoideum.*

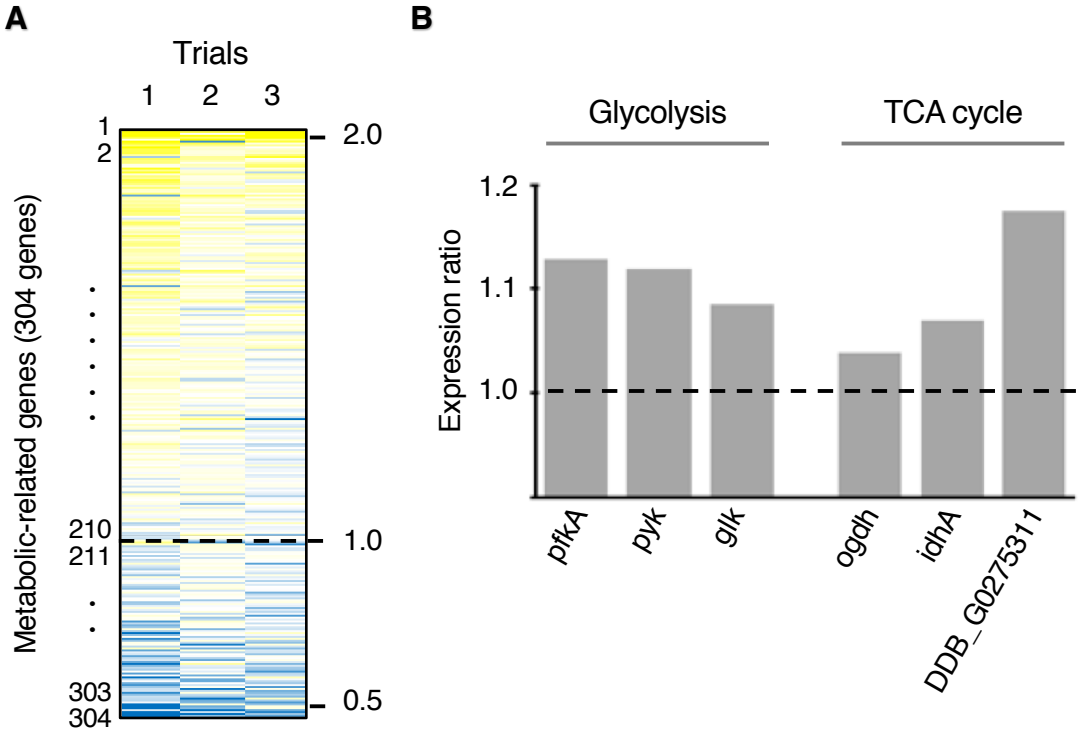

Fig.9 RNA-seq results for metabolism-related genes

(A) The stalk/spore ratio of expression of 304 metabolism-related genes. The color scale is the same as that mentioned in Fig.8**.**

(B) The stalk/spore ratio of expression of genes involved in major energy production. Left 3 and right 3 columns indicate the ratios of genes involved in the glycolysis and TCA cycle, respectively.

Table.2 Genes encoding limiting enzymes in the glycolysis and TCA cycle

List of 10 genes encoding limiting enzymes in the glycolysis and TCA cycle. As several genes involved in the TCA cycle pathway encode same enzyme, most highly expressing genes were selected as representative data shown in the graph of Fig.9B; such genes are marked in the rightmost column. The “FPKM” values indicate the expression levels of each gene provided by NGS service in three RNA-seq measurement. The “Mean ratio” values indicate the mean of the ratios of the expression levels of each gene in the stalk-destined cell to that in the spore-destined cell for three RNA-seq measurement.

Protein name	1st (FPKM)		2nd (FPKM)		3rd (FPKM)		Mean ratio	Fig.9B
	stalk-	spore-	stalk-	spore-	stalk-	spore-		
6-phosphofructokinase	126.99	108.11	137.68	133.22	164.56	140.01	1.13	✓
pyruvate kinase	735.03	595.95	532.47	522.61	673.80	610.28	1.12	✓
glucokinase	35.98	34.39	29.40	26.46	43.99	40.05	1.09	✓
"2-oxoglutarate dehydrogenase, E1 subunit"	168.78	185.38	590.99	517.37	199.63	188.22	1.04	✓
oxoglutarate dehydrogenase	66.84	53.88	93.41	78.99	69.21	58.94	1.20	
isocitrate dehydrogenase (NAD+)	503.16	476.11	1065.15	955.41	501.19	483.59	1.07	✓
isocitrate dehydrogenase (NAD+)	431.80	437.02	665.81	549.86	507.14	448.69	1.11	
"citrate synthase, mitochondrial"	1833.92	1496.73	2570.88	2267.00	2094.84	1797.53	1.17	✓
citrate synthase	85.89	128.37	611.55	579.61	89.72	103.41	0.86	
citrate synthase	47.40	42.65	72.51	63.27	37.09	34.02	1.12	

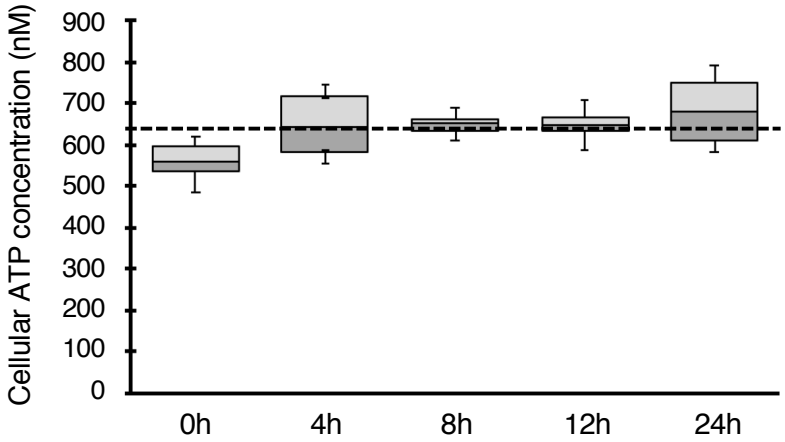

Fig.10 The recovery of cellular ATP concentration from the damage

Cells exposed with the sorting solution for 2 hours were incubated in fresh culture medium for each time duration written in bottom of the graph for the recovery from the damage by sorting solution. Their cellular ATP concentrations after incubation were measured by luciferase assay. The number (n) of measurements; n=16 in all samples. The data is presented as box-and-whisker plots: the box indicates the median and the upper and lower quartiles; the whisker indicates the range. Dashed line indicates the median value of samples incubated for 4 hours.

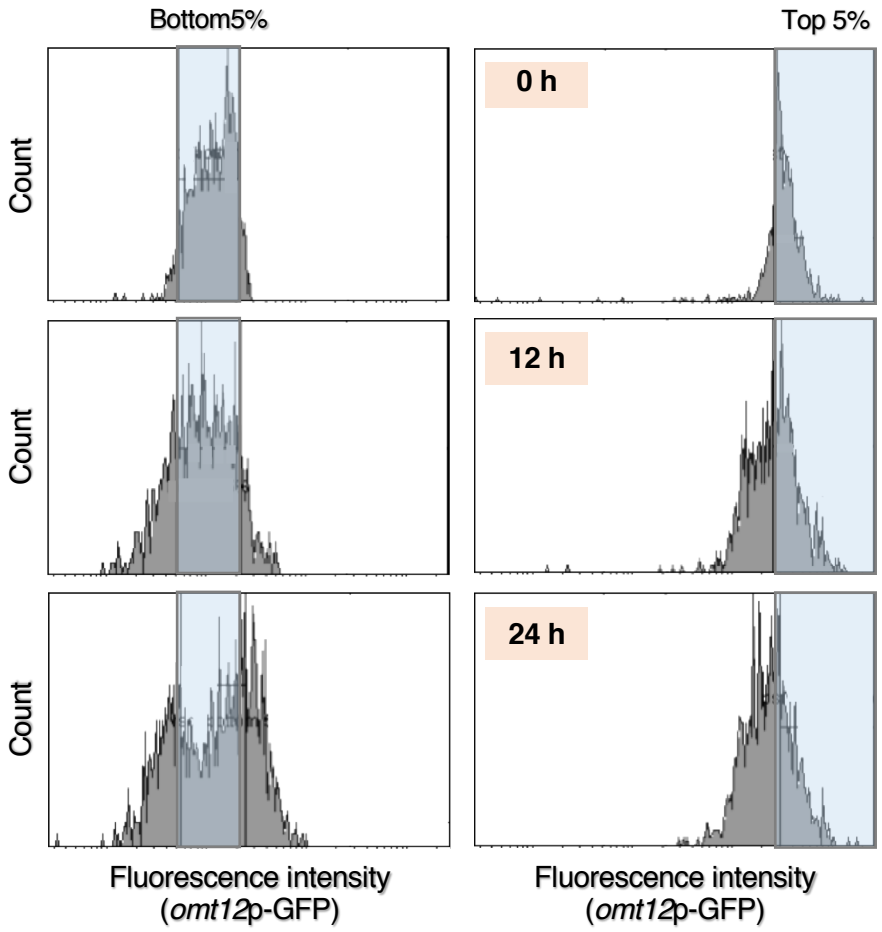

Fig.11 The change of fluorescence distribution of sorted cells

Fluorescence intensity of sorted *omt12*p-GFP cells was measured by flow cytometry after 0h (top panels), 12h (middle panels) and 24h (bottom panels) from sorting. Typical fluorescence intensity distributions of sorted cells of bottom 5% populations (left panel), and top 5% populations (right panel) are shown.

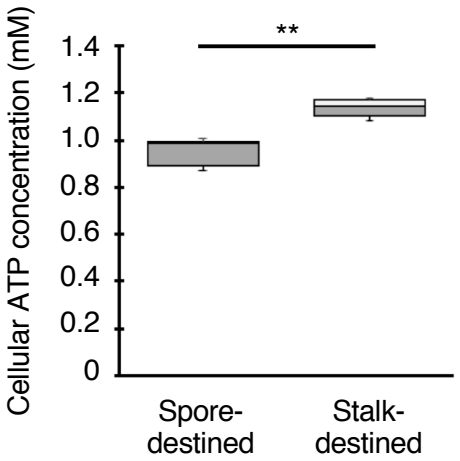

Fig.12 ATP quantification of spore-destined and stalk-destined cells

Cellular ATP concentrations were measured by luciferase assay. The number (n) of measurements; n = 12 (spore-destined) and n = 10 (stalk-destined). The data is presented as box-and-whisker plots: the box indicates the median and the upper and lower quartiles; the whisker indicates the range. Data were analyzed by a unpaired two-tailed Student's t-test. $^{**}p < 0.005$.

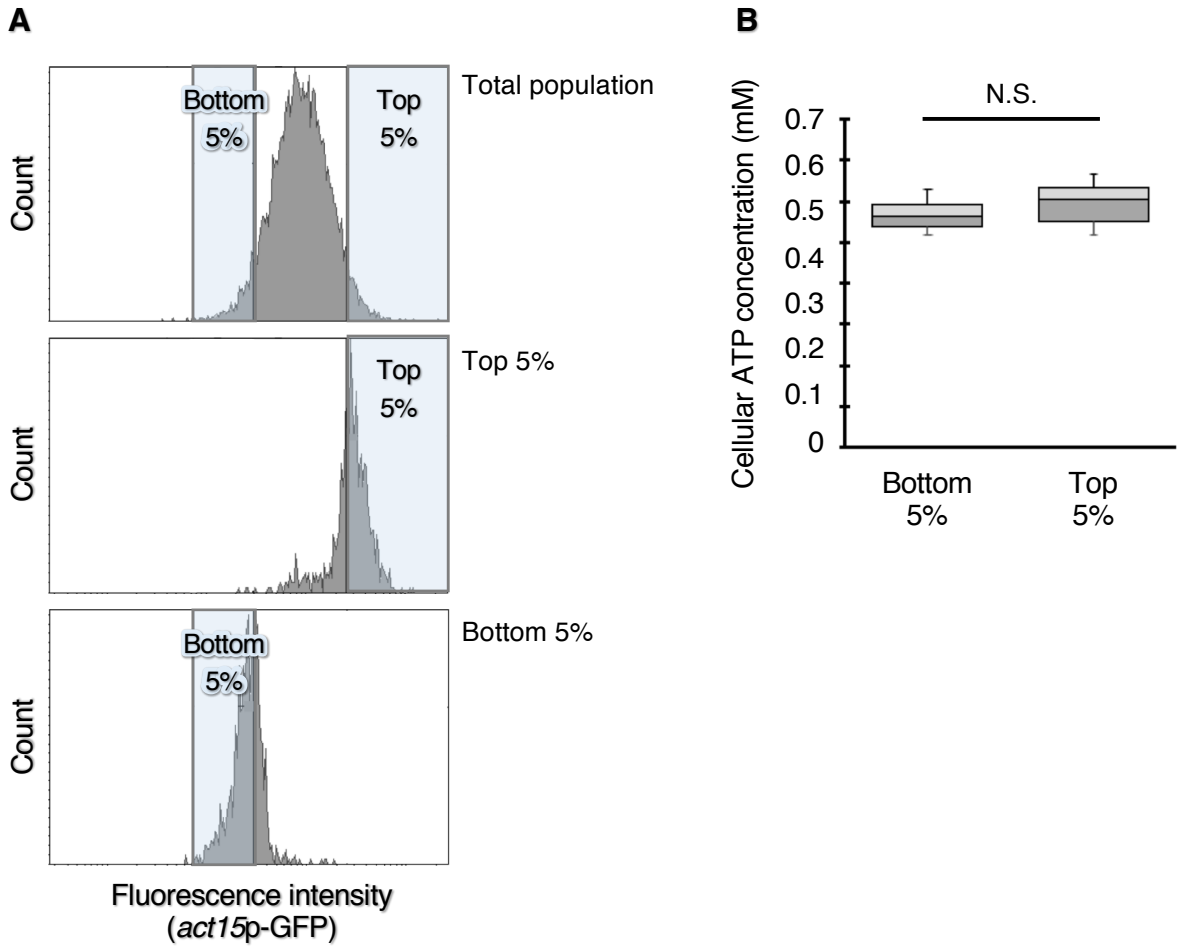

Fig.13 ATP concentrations of cells sorted according to *act15* expression

(A) Fluorescence intensity of *act15*p-GFP cells was measured by flow cytometry before and after sorting to quality-check the cell specimens. Typical fluorescence intensity distributions of total cell population before sorting (top panel), sorted cells of top 5% populations (middle panel), and bottom 5% populations (bottom panel) are shown.

(B) Cellular ATP concentration of sorted *act15*p-GFP cells were measured by luciferase assay. The number (n) of measurements; n = 10 (bottom 5%) and n = 14 (top 5%). The data is presented as box-and-whisker plots: the box indicates the median and the upper and lower quartiles; the whisker indicates the range. Data were analyzed by a unpaired two-tailed Student's t-test. N.S. indicates "Not Significant".

4-3. Visualization of cellular ATP levels by optimized ATP sensor probes

To visualize the ATP levels in *D. discoideum*, MaLionG and AT1.03NL were chosen as the ATP sensor probes working in low-temperature that is suitable for *D. discoideum* culture. MaLionG is an intensiometric indicator consisted of a GFP variant citrine which divided by an ε subunit of the ATP-binding region on the bacterial F_0F_1-ATP synthase (Fig.14A) (Arai et al., 2018). AT1.03NL is a ratiometric FRET probe consisted of a CFP and YFP which divided by same ATP-binding region as MaLionG (Fig.14B) (Imamura et al., 2009; Tsuyama et al., 2013). The codon usages of these indicator probes were optimized based on *D. discoideum* codon usage; each probe was named as DicMaLionG and DicAT1.03NL, respectively. Their intensities decreased when treated by oligomycin, an inhibitor of ATP synthesis, showing that these probes represented the cellular ATP levels in *D. discoudeum* (Fig.15, 16).

However, the alteration of DicAT1.03NL intensity when treated by oligomycin (Fig.16C) and the heterogeneity of the fluorescence intensities at the vegetative phase (Fig.16A, leftmost) were minor compared to those of DicMaLionG (Fig.15). It may be caused by the difference of sensitivities of their original probes: MaLionG and AT1.03NL; AT1.03NL had a little lower sensitivity than MaLionG (see Kd values in Fig.14). My result of luciferase assay (Fig.12) and previous works (Roos et al., 1977) showed that cellular ATP concentration of *D. discoideum* is approximately 1mM: it is lower than that in other organisms (Zimmerman et al., 2011). As a little difference of sensitivities between MaLionG and AT1.03NL will be critical in *D. discoideum* with lower ATP levels, ATP visualization by DicAT1.03NL may be difficult. Therefore, DicMaLionG was mainly used hereafter and DicAT1.03NL was used only for important experiments that should be confirmed by both probes.

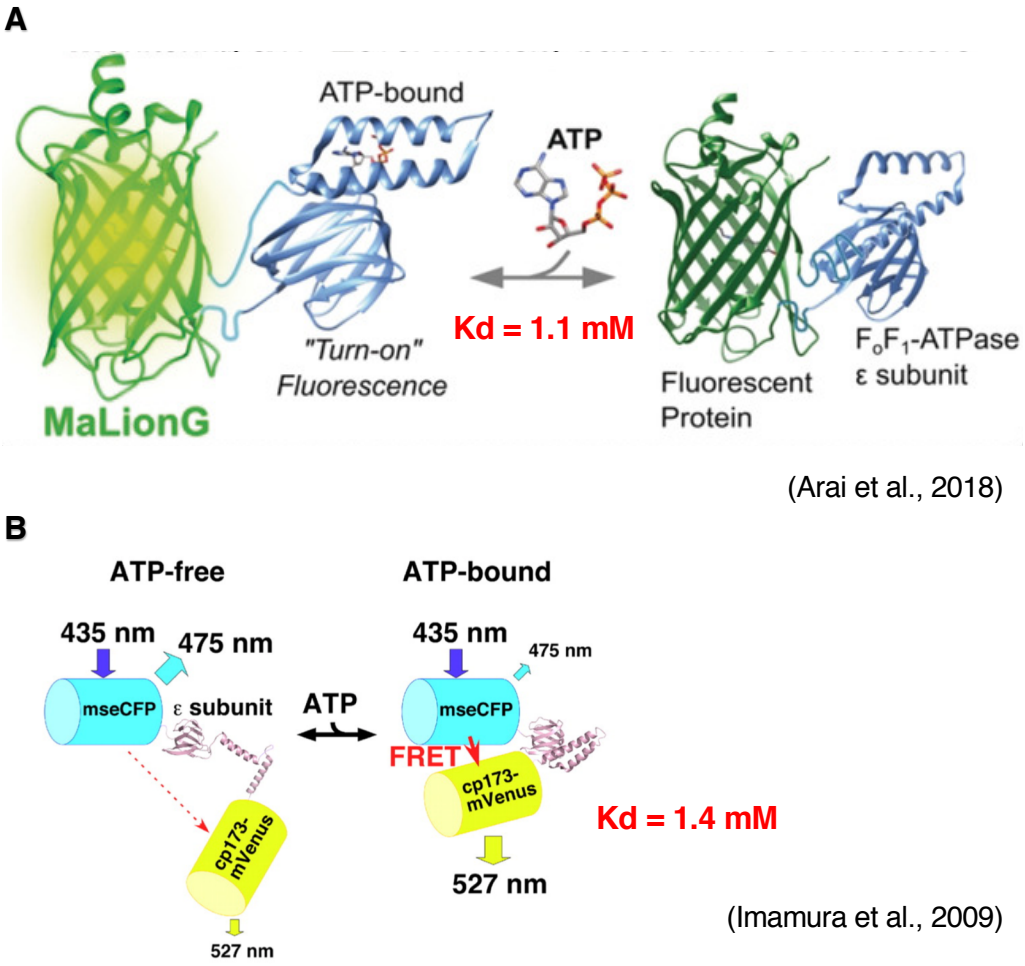

Fig.14 Schematic images of ATP sensor probes

(A) Schematic image of MaLionG (Arai et al., 2018). Left-side and right-side images represent the condition with ATP-bound and with ATP-free, respectively. GFP fluorescence can be observed when ATP-bound.

(B) Schematic image of AT1.03NL (Imamura et al., 2009). Left-side and right-side images represent the condition with ATP-free and with ATP-bound, respectively. CFP fluorescence is observed when ATP-free and YFP fluorescence as a result of FRET is observed when ATP-bound. ATP level is indicated by the ratio of their fluorescence intensity (YFP/CFP).

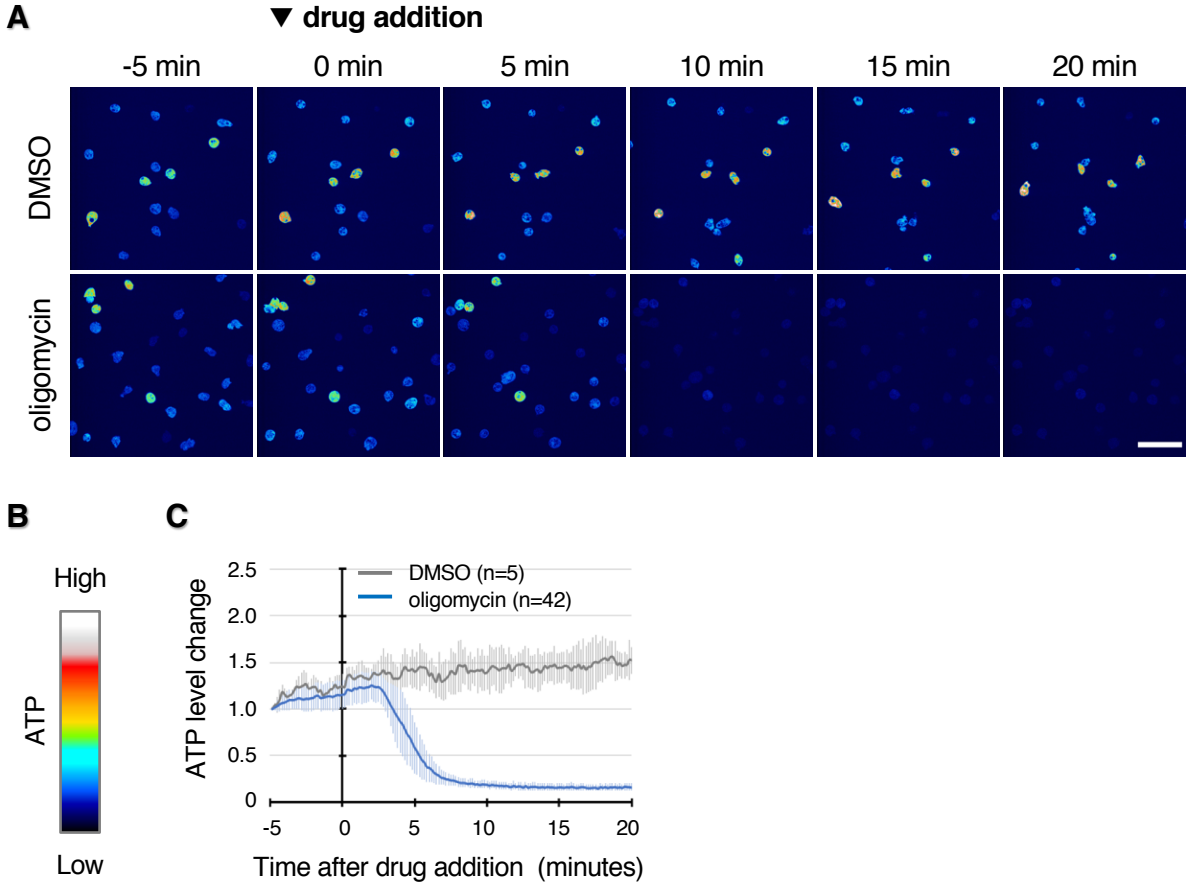

Fig.15 Evaluation of DicMaLionG as an ATP sensor probe

(A) Fluorescence images of DicMaLionG. The amoeba cells were treated with oligomycin (bottom panels) and dimethyl sulfoxide (DMSO) as a control solvent (top panels) for indicated time periods. Images were acquired every 10 seconds by Dragonfly200 using a 60× oil immersion objective lens. Scale bar, 50 μm.

(B) The fluorescence intensity (ATP level) of cells in (A) are indicated by this color scale.

(C) Changes in fluorescence intensity (ATP level) over time during drug treatment. Changes in fluorescence intensity were measured over time for individual cells by Fiji. The rate of change was plotted with the intensity at the start (−5 min) as 1. Gray and blue lines indicate DMSO and oligomycin treatment, respectively. The number (n) of analyzed cells; oligomycin (n = 42) and DMSO (n = 5). Mean and SD are shown.

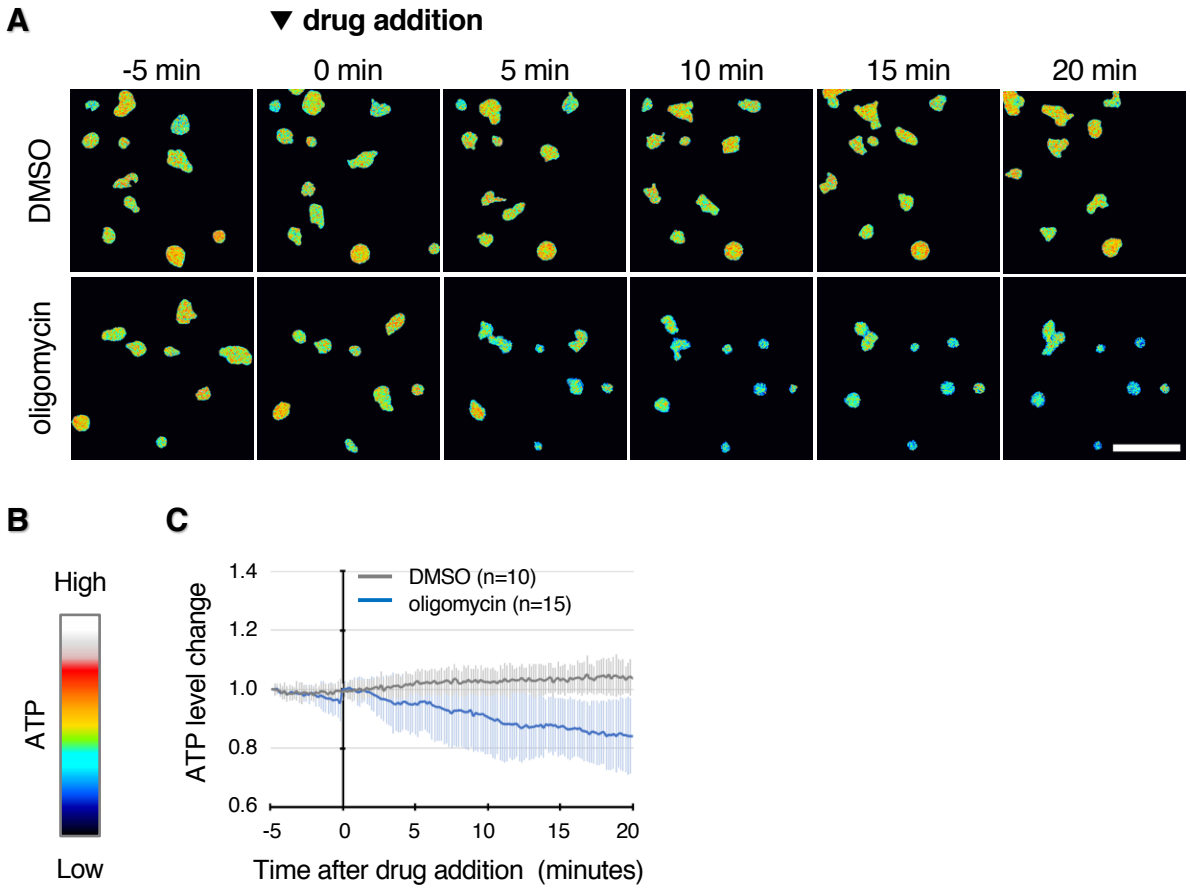

Fig.16 Evaluation of DicAT1.03NL as an ATP sensor probe

(A) Fluorescence images of DicAT1.03NL. The amoeba cells were treated with oligomycin (bottom panels) and DMSO as a control solvent (top panels) for indicated time periods. These are ratio images depicting the values of YFP/CFP intensity (see Materials and Methods section for details). Images were acquired every 10 seconds by LSM780 using a 63×oil immersion objective lens. Scale bars, 50 μm.

(B) The fluorescence intensity (ATP level) of cells in (A) are indicated by this color scale.

(C) Changes in YFP/CFP ratio (ATP level) over time during drug treatment. Changes in YFP/CFP ratio were calculated over time for each cell. The rate of change was plotted with the intensity ratio at the start (−5 min) as 1. Blue and gray lines indicate oligomycin and DMSO treatment, respectively. The number (n) of analyzed cells; oligomycin (n = 15) and DMSO (n = 10). Mean and SD are shown.

4-4. Correlation between *omt12* expressions and ATP levels

As DicMaLionG probe enabled me the visualization of cellular ATP levels in *D. discoideum,* I investigated the correlation between *omt12* expressions and ATP levels by microscopic observation using *omt12*p-mCherry/DicMaLionG cells in order to confirm the result of luciferase assay. Observation of these cells at the vegetative phase showed that the intensities of *omt12*p-mCherry and that of DicMaLionG (ATP level) were high correlated (Fig.17A). I also observed the cells expressing *act15*p-mRFPmars instead of *omt12*p-mCherry as a control. In this case, the intensities of *act15*p-mRFPmars and DicMaLionG showed no correlation (Fig.17B). These observation at the vegetative phase showed that *omt12* expressions and ATP levels were high correlated also in physiological condition, confirming the result that stalk-destined cells (highly expressing *omt12*) had higher ATP levels than spore-destined cells (low expressing *omt12*).

The correlation between *omt12* expressions and ATP levels was also observed at various developmental stages using *omt12*p-mCherry/DicMaLionG cells. For easy analysis of correlation, only 1% fluorescent cells were mixed to wild-type Ax2 cells with no fluorescence. Results showed that *omt12* expressions and ATP levels were highly correlated at all stages including vegetative phase, aggregation phase, loose/tight mound phase, and slug phase (Fig.18). This high correlation throughout the developmental process suggested that the ATP levels of stalk-destined cells are kept higher during development, until the differentiation to stalk cells.

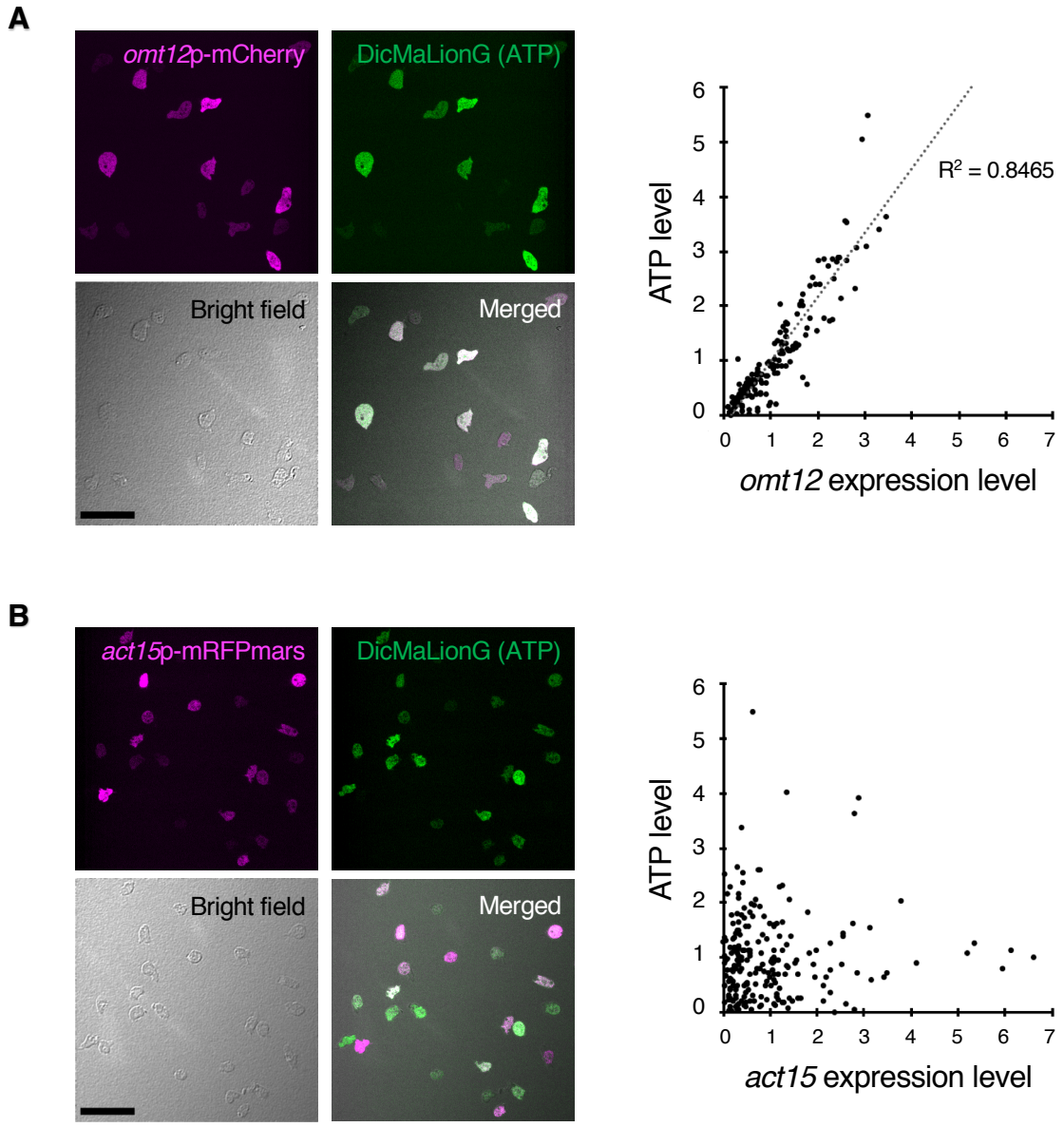

Fig.17 Correlation between *omt12* and ATP levels at the vegetative phase

(A) Images of cells of the *omt12*p-mCherry/DicMaLionG double-expressing strain: *omt12*p-mCherry (magenta), DicMaLionG (ATP) (green), a bright field image, and the merged image as indicated in the panels. These images were acquired by FV1000 using a 60× oil immersion objective lens. Scale bar, 50 μm. The graphs indicate plots of the values obtained by measuring the intensity of each cell and dividing by the mean intensity; the line indicates the linear regression of the plots. The number (n) of cells: n=190.

(B) Images of cells of the *act15*p-mRFPmars/DicMaLionG double-expressing strain: *act15*p-mRFPmars (magenta), DicMaLionG (ATP) (green), a bright field image, and the merged image as indicated in the panels. These images were acquired by FV1000 using a 60× oil immersion objective lens. Scale bar, 50 μm. The graphs indicate plots of the values obtained by measuring the intensity of each cell and dividing by the mean intensity. The number (n) of cells: n = 214.

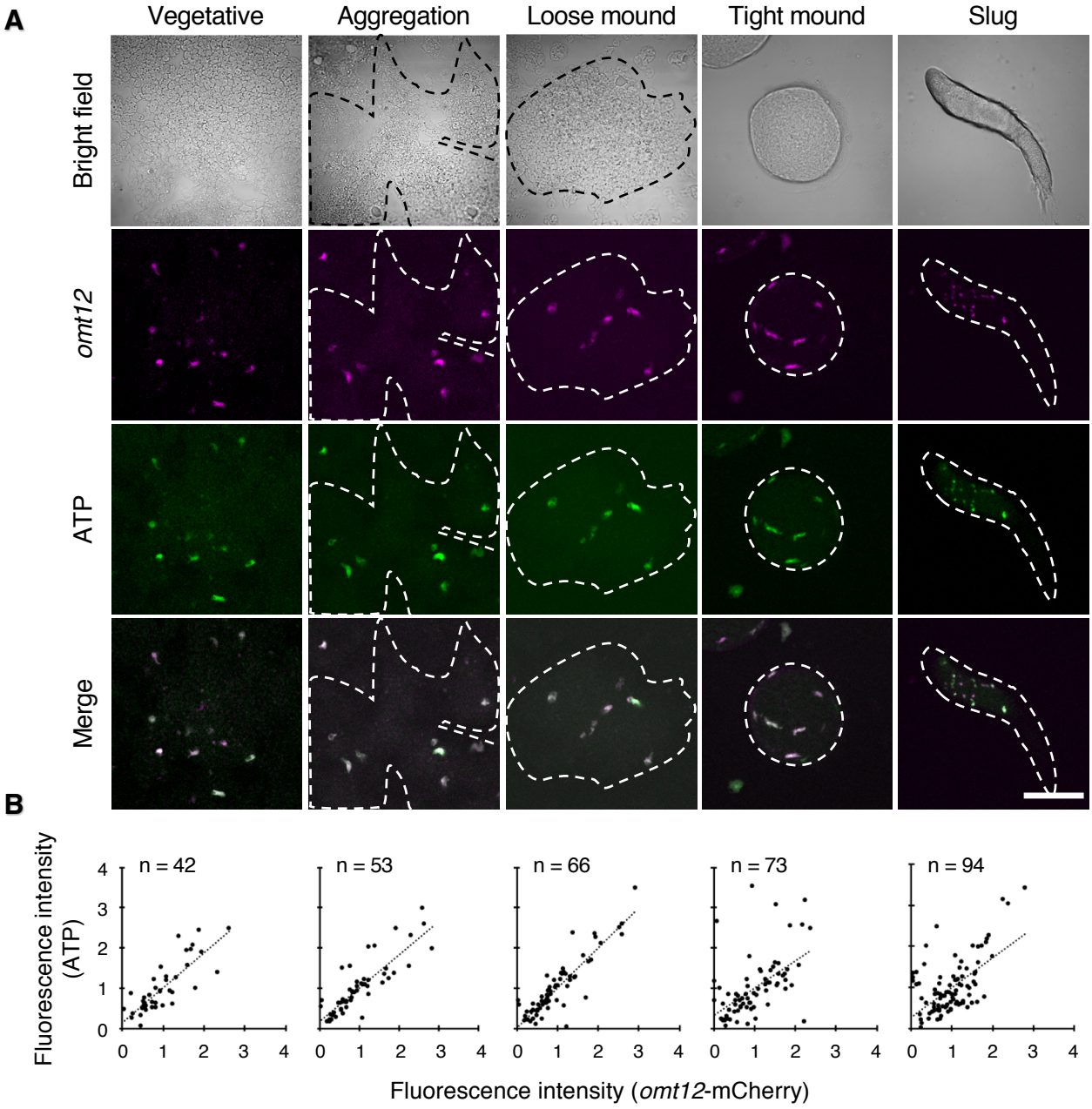

Fig.18 Correlation between *omt12* and ATP levels during development

(A) Cells expressing *omt12*p-mCherry (magenta) and DicMaLionG (ATP; green) were mixed with wild-type Ax2 cells (not expressing fluorescent protein) at a ratio of 1%, and the process of development was observed. Bright-field images (top), fluorescence images of *omt12*p-mCherry (second row), that of DicMaLionG (third row), and their merged images (bottom) are shown. Dashed lines indicate the periphery of cellular population. These images were obtained by FV1000 using a 40× objective lens. Scale bars, 50 μm.

(B) Lower graphs indicate the correlation between two fluorescent proteins. The graph indicates the plots of the values obtained by measuring the intensity of each cell and dividing by the mean intensity; the lines indicate the linear regression of the plots. The number (n) of the cells tested is indicated in each graph.

4-5. Higher ATP levels of stalk cells throughout the developmental process

In order to investigate the ATP levels of stalk-destined cells and stalk cells in the developmental process, I observed the various developmental stages using DicMaLionG cells including vegetative phase, mound phase, slug phase, culminant phase, and fruiting body phase. Results showed that cells localized in the anterior prestalk region of a slug and in the stalk cells of a fruiting body had actually higher ATP levels (Fig.19A). To further confirm this result, a FRET-type ATP sensor probe, DicAT1.03NL, was used. DicAT1.03NL revealed a similar localization pattern as that observed when using DicMaLionG (Fig. 19B). In contrast, control cells expressing *act15*p-mRFPmars showed a diffuse distribution throughout the multicellular body at various stages of development (Fig. 19C). Taken together with the result of ATP quantification at the vegetative phase, it was shown that stalk cells kept higher ATP levels throughout the developmental process from before differentiation, suggesting that cells with higher ATP levels at the vegetative phase differentiate into stalk cells later.

To confirm it directly, we tracked the ATP-rich cells from the vegetative phase until slug formation by observing the developmental process of the mixed cell population of DicMaLionG cells and wild-type Ax2 cells. This observation duration is enough to identify the fate of cells, as cells localized at anterior prestalk region of a slug normally differentiate into stalk cells later. As a control, ATP-poor cells were also tracked. First, I observed the aggregation process from the vegetative phase to the mound phase; DicMaLionG cells were mixed 5% here. Both ATP-rich cells and ATP-poor cells aggregate to form a mound with keeping their initial intensities (Fig.20). At this point, neither of them localized at specific region in a mound (Fig.20A). Second, I observed the process of slug formation from a mound contained DicMaLionG cells with 1%. Here, ATP-rich cells first moved rotationally along the edge of a mound until slug formation,

and then moved toward the anterior prestalk region of a slug (see red lines in “1:30” - “2:30” of Fig.21). ATP-poor cells moved rotationally as same with ATP-rich cells at first. However, they did not reach the anterior prestalk region and stayed at the middle region (spore region) of a slug (see green and purple lines in “1:30” - “2:30” of Fig.21). These observations support the hypothesis that the ATP-rich cells at the vegetative phase differentiate into stalk cells.

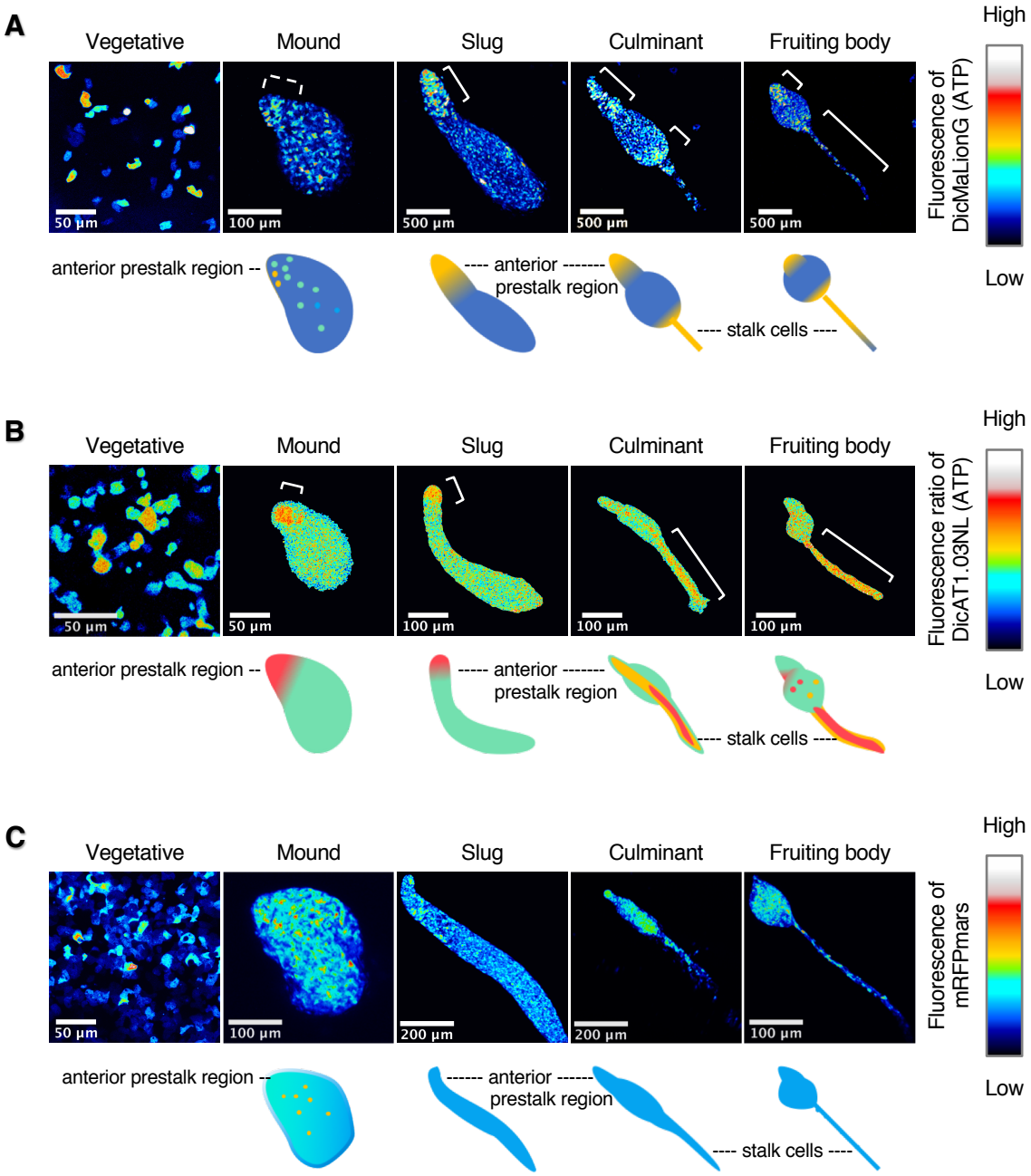

Fig.19 Imaging of ATP levels during development

Fig.19 Imaging of ATP levels during development

(A) Typical fluorescence images of DicMaLionG in each stage of development (upper panels), and schematics of the corresponding developmental stages (bottom). The DicMaLionG expressing strain was used. ATP levels are indicated by the color scale presented on the right. White lines indicate cells with high fluorescence intensity. Images were acquired by FV1000 and projected with the maximum intensity of z-stack images using Fiji. Objective lenses used: 60× oil immersion lens for vegetative cells; 40× lens for the mound; and 20× lens for the slug, culminant, and fruiting body.

(B) Typical FRET ratio images of DicAT1.03NL in each stage of development (upper panels), and schematics of the corresponding developmental stages (bottom). The DicAT1.03NL expressing strain was used. ATP levels are indicated by the color scale presented on the right. White lines indicate cells with high fluorescence intensity. Images were acquired by LSM780 and projected with the maximum intensity of z-stack images using Fiji. Objective lenses used: 60× oil immersion lens for vegetative cells; 40× lens for the mound; and 20× lens for the slug, culminant, and fruiting body.

(C) Typical fluorescence images of act15p-mRFPmars in each stage of development (upper panels), and schematics of the corresponding developmental stages (bottom). The act15p-mRFPmars expressing strain was used. Expression levels of *act15*p-mRFPmars are indicated by the color scale presented on the right. Images were acquired by FV1000 and projected with the maximum intensity of z-stack images using Fiji. Objective lenses used: 60× oil immersion lens for vegetative cells; 40× lens for mound; 20× lens for slug and culminant; 40× lens for the fruiting body.

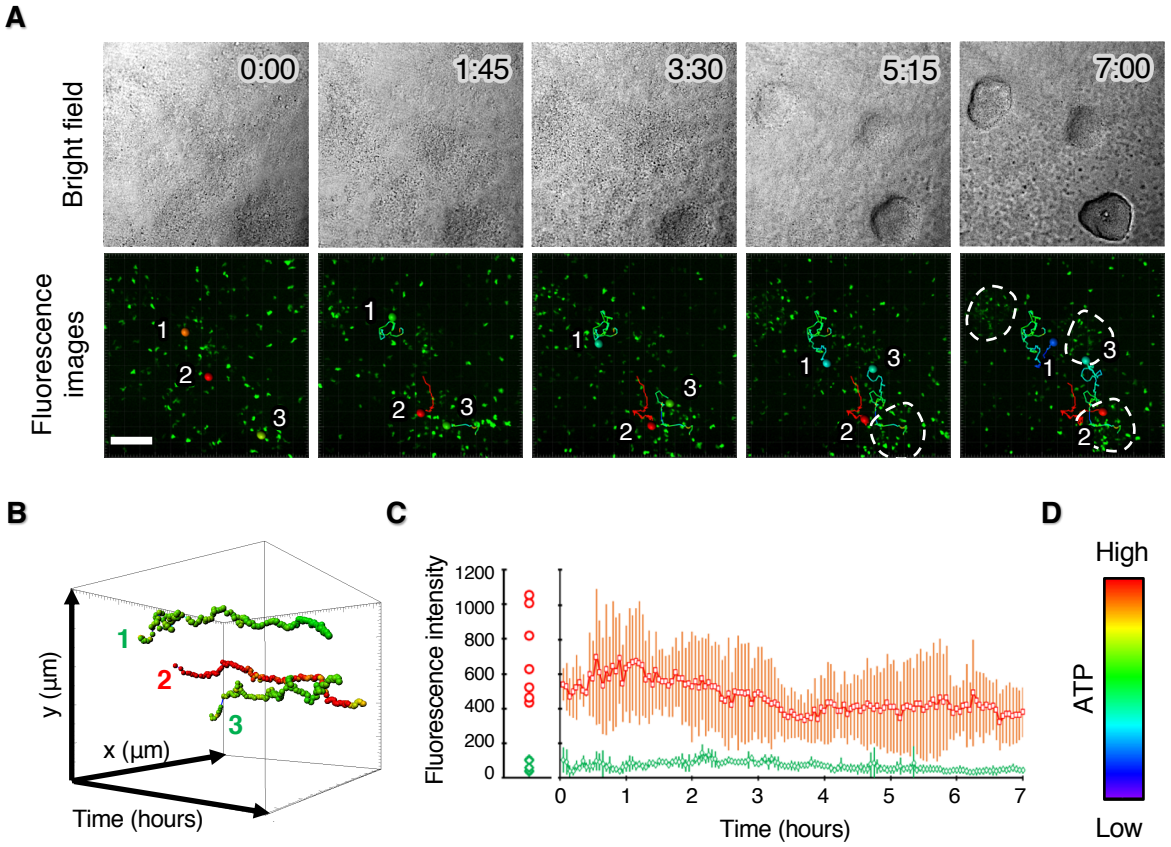

Fig.20 Tracking of cells in the aggregation process

(A) Tracking of single cells of interest during development from the vegetative phase to the mound phase. Upper and middle panels indicate bright-field and fluorescence images, respectively. Z-stack images were acquired every 3 minutes by Dragonfly200 using a 20 × objective lens and projected with the maximum intensity using Fiji. The number in each image indicates time in hours:minutes. Representative trajectories of three individual cells are shown in the fluorescence images; their colors represent the fluorescence intensity (ATP level) of individual cells as the color scale in (D). Dashed lines indicate the periphery of mounds. Scale bar, 100 μm.

(B) This 3D graph shows the trajectories of three cells indicated in (A) over time; their colors represent the fluorescence intensity as same.

(C) This graph indicates the plots of mean fluorescence intensity of all tracked cells with high ATP levels (red) and low ATP levels (green); mean and SD is plotted over time (n = 7 and n = 5 for high and low ATP levels, respectively). Initial intensity of each cell is shown at the left of the graph.

(D) The fluorescence intensity (ATP level) of cells in (A) and (B) are indicated by this color scale.

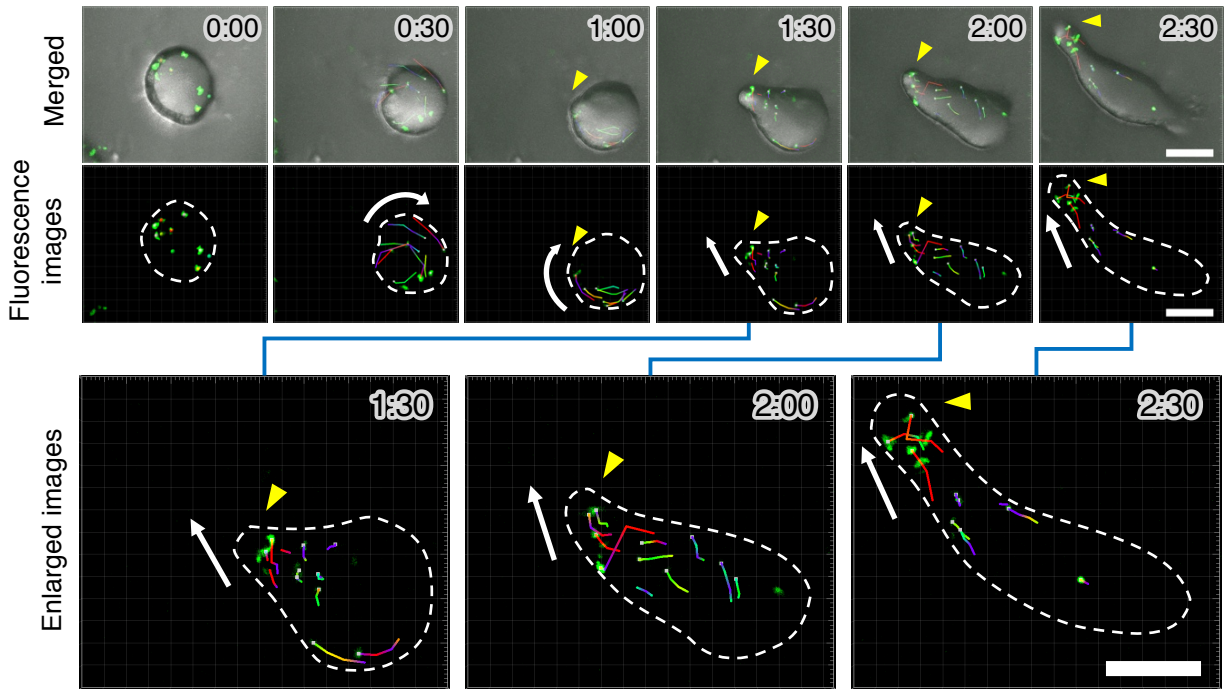

Fig.21 Tracking of cells in the process of slug formation

Tracking of single cells of interest during development from the mound phase to the slug phase. Upper panels indicate the merged images of bright-field and fluorescence images, and middle panels indicate the fluorescence images with trajectories over time. The number in each image indicates time in hours:minutes. Z-stack images were acquired every 3 minutes by Dragonfly200 using a 20× objective lens. The color of trajectories represent their intensity as same in Fig.20D. Bottom panels indicate the enlarged images of right 3 images of the middle panels. Yellow arrowheads indicate where the anterior prestalk region was formed. White arrows indicate moving direction of cells. Scale bar, 100 μm.

4-6. Changes of cell fates from stalk-destined cells into spore cells

In order to understand the importance of ATP in cell differentiation, I tried to reduce the cellular ATP concentrations of stalk-destined cells at the vegetative phase and observe the future cell fates. For reducing the cellular ATP concentrations, two drugs were chosen as inhibitors of ATP synthesis (Fig. 22A): 3-bromopyruvic acid (3-BrPA; an inhibitor of enzyme activity of hexokinase II and a rate-limiting and critical enzyme of glycolysis) (Ko et al., 2001; Geschwind et al., 2002) and oligomycin (an inhibitor of ATP synthase activity in mitochondria) (Chappell and Greville, 1961; Kim and Berdanier, 1999; Cunningham and George, 1974). The cellular ATP concentrations of stalk-destined cells at the vegetative phase sufficiently reduced to equal as or lower than that of spore-destined cells by treatment of these inhibitors (Fig.22B). Under the same condition, stalk-destined cells (highly expressing *omt12*p-GFP) were treated by 3-BrPA or oligomycin to reduce their cellular ATP concentrations. Treated stalk-destined cells were mixed at a ratio of 2:8 with untreated wild-type Ax2 cells with no fluorescence to accommodate for development initiation, and the fates of those treated stalk-destined cells were observed at the slug phase and the fruiting body phase.

First, I observed the fates of the treated stalk-destined cells (highly expressing *omt12*p-GFP) in a slug. In the control, the untreated stalk-destined cells localized in the anterior prestalk region of a slug as expected (Fig.23A, left). In contrast, stalk-destined cells treated by 3-BrPA or oligomycin did not localize in the anterior prestalk region, but scattered throughout the slug (Fig.23A, middle and right). For the analysis of localization of stalk-destined cells, slug was divided into 10 sections from the anterior region to the posterior region so that each section has almost same area. Then GFP fluorescence intensity in each section was measured by fiji software and normalized values by dividing by the mean intensity of all 10 sections were plotted (Fig.23A, bottom). These graphs

also demonstrated that untreated stalk-destined cells as a control had strong GFP localization in the anterior prestalk region, whereas treated stalk-destined cells lost their localization. Next, I observed the fates of treated stalk-destined cells in a fruiting body. In the control, the untreated stalk-destined cells differentiate into stalk cells as expected and GFP fluorescence was not observed in the spore region (Fig.23B, left). In contrast, GFP fluorescence of stalk-destined cells treated by 3-BrPA or oligomycin were not observed in stalk region but in spore region of a fruiting body (Fig.23B, middle and right), suggesting that they changed the cell fates from stalk cells to spore cells. Two inhibitors working in different pathways, glycolysis and mitochondrial ATP synthesis, showed similar results. As the common goal of these pathways is the production of ATP molecule, it is possible that the changes of cell fates was caused by the reduce of ATP levels by the treatment of these inhibitors. These results demonstrated that ATP influences the cell fate determination in *D. discoideum* differentiation.

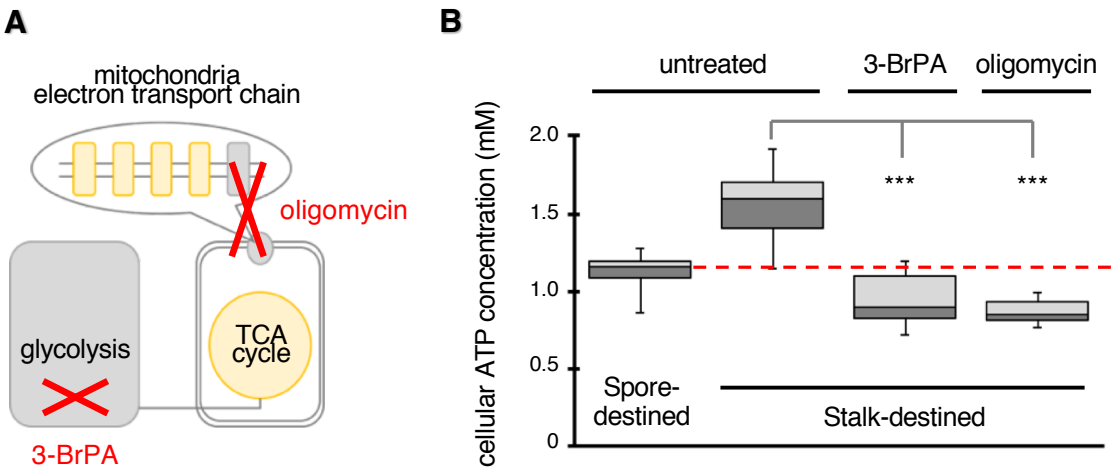

Fig.22 The effects of two drugs to inhibit the ATP synthesis

(A) Schematic diagram showing the reaction sites where each inhibitor has an effect. 3-BrPA inhibits the limiting enzyme (hexokinase II) activity in glycolysis, and oligomycin inhibits an ATP synthase required for ATP production in mitochondria.

(B) Cellular ATP concentration in the cells untreated or treated with drugs as measured by luciferase assay. The red dashed line represents the median value of cellular ATP concentration in untreated spore-destined cells. The number of specimens tested; n = 27, 28, 15, and 13 from the left. The data is presented as box-and-whisker plots: the box indicates the median and the upper and lower quartiles; the whisker indicates the range. Data were analyzed by the unpaired two-tailed Student's t-test. ***$p < 0.001$.

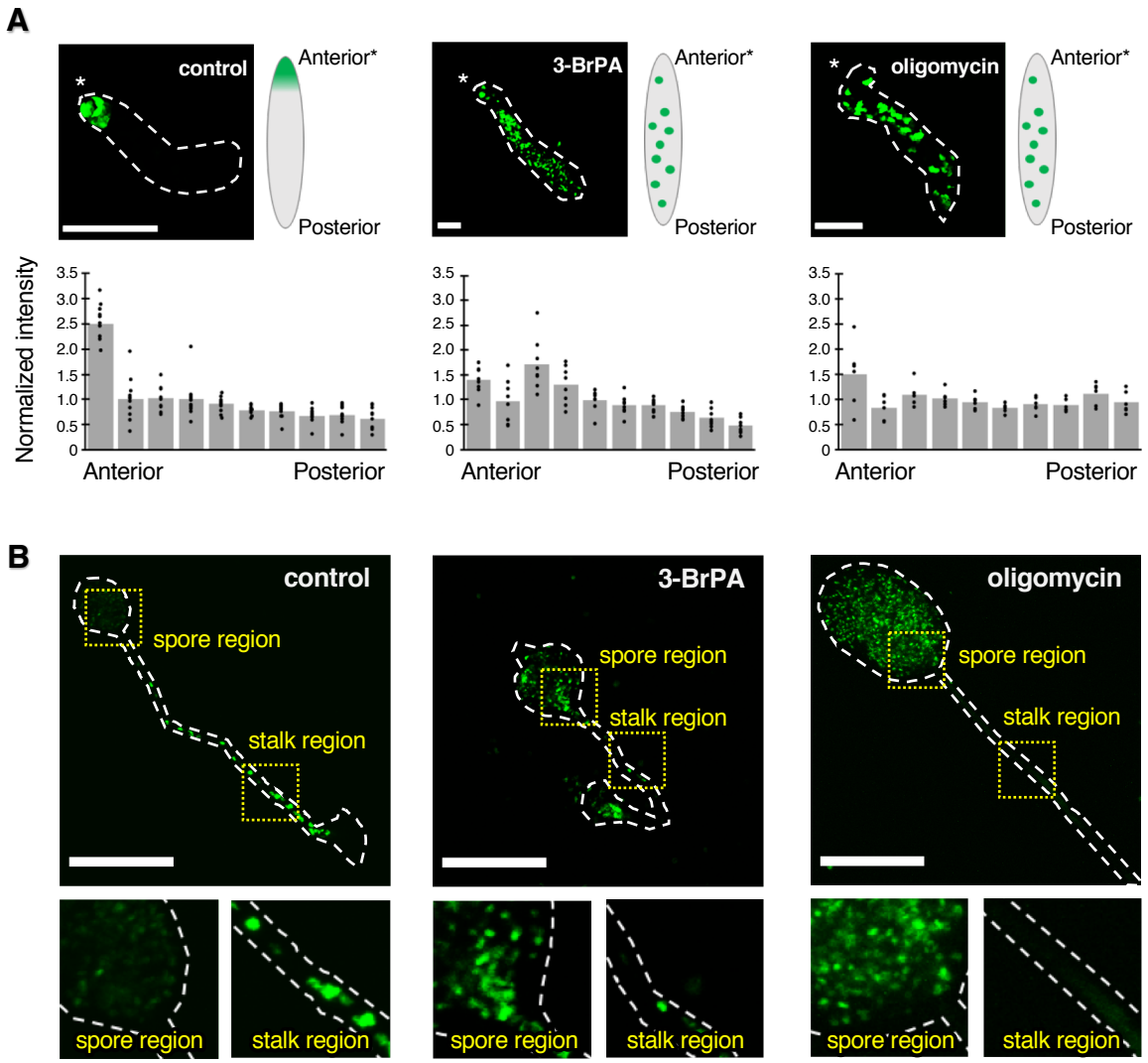

Fig.23 The cell fate of ATP-reduced stalk-destined cells

(A) Fluorescence images of *omt12*p-GFP in a slug. The stalk-destined cells collected using a cell sorter were untreated (control, left panel) or treated with 3-BrPA (middle panel) or oligomycin (right panel) and mixed at a 2:8 ratio with wild-type Ax2 cells (not expressing GFP) for observing their cell fates. Dashed lines indicate the periphery of a slug. The schematic diagram on the right of each image shows an overview of the results obtained. These images were acquired by FV1000 using a 20× objective lens and projected with the maximum intensity of z-stack images by Fiji. The lower graphs show the GFP fluorescence intensity quantified in each section obtained by dividing the slug into 10 sections from the anterior to the posterior. Each section was divided to have the same area. The values were calculated as (intensity of each section)/(mean intensity of 10 sections). The number of samples tested, n = 11, 8, and 6 from the left. Scale bars, 50 μm.

(B) A fruiting body observed in the same manner as (A). Dashed lines indicate the periphery of a fruiting body. The spore regions and stalk regions indicated by dotted squares are enlarged and displayed in the lower panels. These images were acquired by FV1000 using a 20× objective lens and projected with the maximum intensity of z-stack images by Fiji. Scale bars, 100 μm.

4-7. The regulation of cell fates of differentiation by relative ATP levels

The hypothesis that ATP influences the cell fate determination raises the further question about the mechanism. I wonder which is important to regulate the cell fates: the absolute value of cellular ATP concentration or the relative value. In order to reveal this question, ATP-rich cells (top 5% fluorescence intensity of DicMaLionG) and ATP-poor cells (bottom 5% fluorescence intensity of DicMaLionG) were separately collected by a cell sorter, and then starved independently to induce development. In a case that absolute value is important, all of cells contained in the top 5% populations are expected to differentiate into stalk cells, whereas those in the bottom 5% populations will differentiate into spore cells. In contrast, when differentiation is regulated by relative value, cells with higher ATP levels and those with lower ATP levels in each population are expected to differentiate into stalk and spore cells, respectively; normal fruiting body will be formed in this case. As a result, both ATP-rich cells and ATP-poor cells finally formed a normal fruiting body, but the formation of fruiting body was largely delayed in comparison with wild-type Ax2 cells as a control (Fig.24). Furthermore, ATP levels were a little higher in the anterior prestalk region of a slug composed of ATP-rich cells (Fig.25, top). Difference in ATP levels was not detected in a slug composed of ATP-poor cells (Fig.25, bottom), however it may be due to insufficient sensitivity of DicMaLionG probe to detect subtle difference. These results suggest that relative ATP level among cells is important to affect the cell fates of differentiation.

However, in addition to the delay of formation, strange structures of fruiting bodies were also observed in both ATP-rich and ATP-poor cell populations (Fig.26). In the ATP-rich cell population (top 5%), it appeared that a part of the posterior prespore region of a slug was left behind during the formation of a fruiting body (Fig.26B, left). In the ATP-poor cell population (bottom 5%), it appeared that stalk cells were abnormally

formed from a slug (Fig.26B, right). These results demonstrated the possibility that the differentiation into spore or stalk cells turned difficult in the top 5% and the bottom 5% cell populations, respectively. Taken together, it is plausible that the cell fates can be basically regulated by relative ATP levels, but it possibly needs the somewhat wide distribution of ATP levels for the smooth proceeding of differentiation.

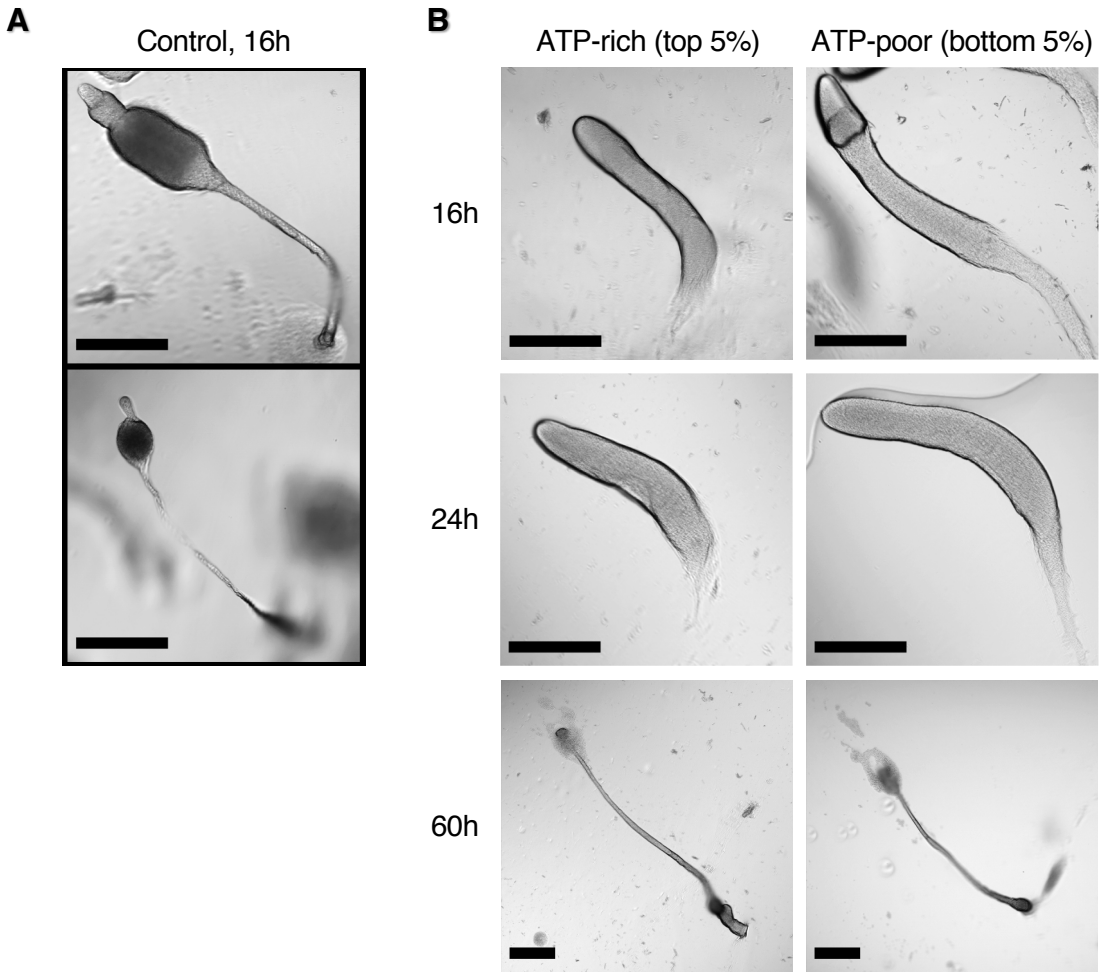

Fig.24 The developmental process of ATP-rich and ATP-poor cell population

(A) Representative bright-field images of wild-type Ax2 cells as a control which were observed 16 hours later from development initiation. These images were acquired by FV1000 using a 20× objective lens. Scale bars, 200 μm.

(B) Representative bright-field images of ATP-rich (left) and ATP-poor (right) cell populations which were sorted according to fluorescence intensity of DicMaLionG (ATP level). Images observed 16 hours later (top panels), 24 hours later (middle panels) and 60 hours later (bottom panels) are shown. These images were acquired by FV1000 using a 20× objective lens (16 hours and 24 hours) and a 10× objective lens (60 hours). Scale bars, 200 μm.

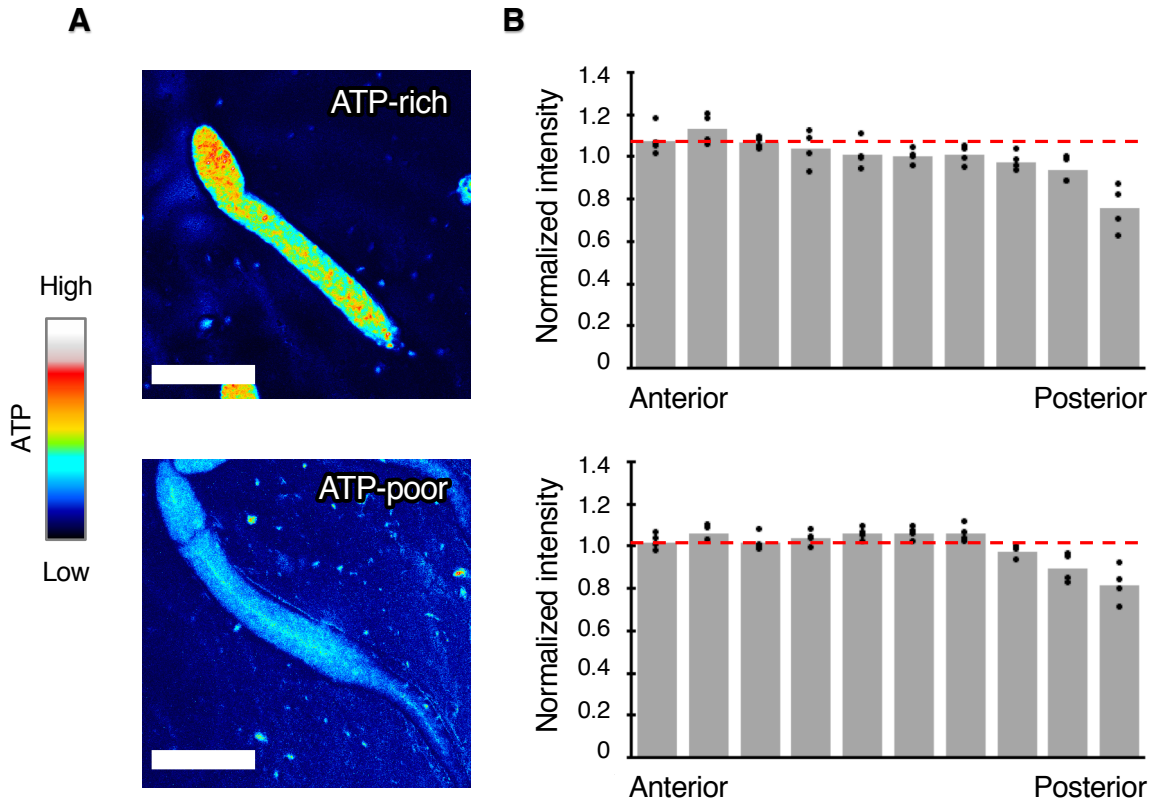

Fig.25 ATP distribution in a slug composed of ATP-rich or ATP-poor cells

(A) Representative fluorescence images of ATP-rich (top panel) and ATP-poor (bottom panel) cell population. Their intensities (ATP levels) are indicated by the color scale given on the left. These images were acquired by FV1000 using a 20× objective lens. Scale bars, 200 μm.

(B) The graphs show the fluorescence intensity quantified in each section obtained by dividing the slug into 10 sections from the anterior to the posterior. Each section was divided to have the same area. The values were calculated as (intensity of each section)/(mean intensity of 10 sections). Red dashed lines indicate the mean values of most anterior region (leftmost box in the graph). The number of samples tested, n = 4 for both.

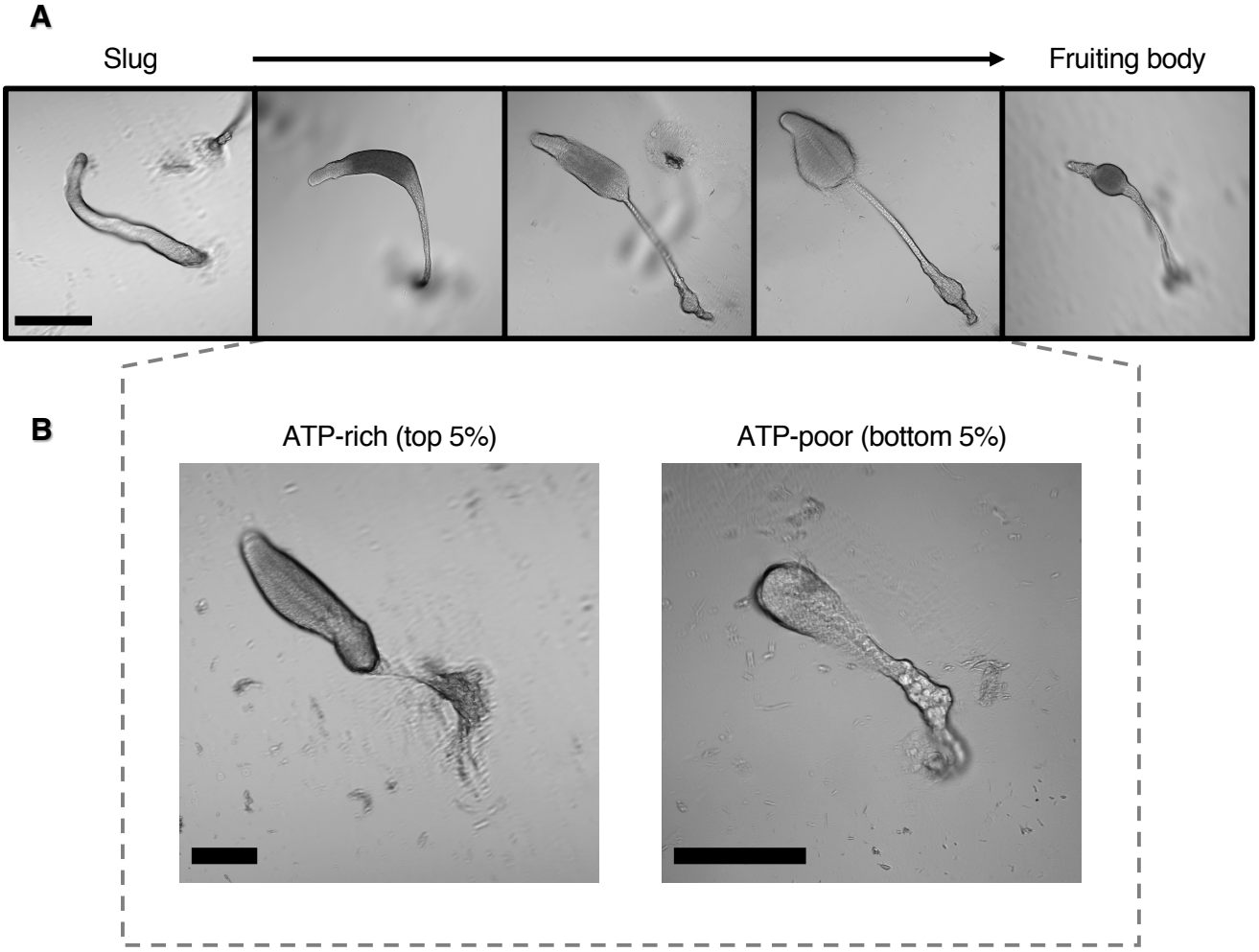

Fig.26 The strange fruiting body in ATP-rich and ATP-poor cell population

(A) Bright-field images of wild-type Ax2 cells as a control, showing the typical process of a fruiting body formation from a slug. These images were acquired by FV1000 using a 20× objective lens. Scale bars, 200 μm.

(B) The fruiting bodies which observed in ATP-rich (left) and ATP-poor (right) cell population. The strange structures compared with control images shown in (A) were observed in both ATP-rich and ATP-poor cell population during fruiting body formation. These images were acquired by FV1000 using a 20× objective lens (ATP-rich cell population) and a 40× objective lens (ATP-poor cell population). Scale bars, 100 μm.

4-8. cAMP as a differentiation factor possibly affected by ATP

Then, what is the role of ATP for regulating the differentiation? I wonder why ATP-rich cells and ATP-poor cells differentiate into stalk and spore cells, respectively. As described in chapter 2-2, stalk cells are differentiated from prestalk cells which are localized at the anterior region of a slug. Those spatial information is also important for differentiation and the sorting mechanism of prestalk cells to the tip region have been discussed for long time. It has been proposed that the different characteristics of prestalk and prespore cells, the levels of cell motility and of cAMP chemotaxis, induce the sorting of stalk cells (Traynor et al., 1992; Abe et al., 1994; Early et al., 1995; Rietdorf et al., 1996; Fujimori et al., 2019). Therefore, I investigated the influence of ATP level to the cell motility and the cAMP chemotaxis efficiency.

As an ATP is a molecule working as energy resource, ATP-rich cells may be able to move faster and reach the anterior prestalk region of a slug. To prove this hypothesis, I first compared the motilities of ATP-rich cells and ATP-poor cells during development. The speed and the ATP level (fluorescence intensity of DicMaLionG) were analyzed based on the previous cell tracking results in the aggregation process (see the images in Fig.20) and in the process of slug formation (see the images in Fig.21). In the aggregation process, the speed and the ATP level showed no correlation (Fig.27A). Although there seemed to be the positive correlation between the speed and the ATP level in the process of slug formation (Fig.27B), they were not correlated statistically.

On the other hands, the observations of this slug formation process provided me interesting finding that ATP-rich cells suddenly changed their moving direction just before the anterior prestalk region was formed (see “0:51” of Fig.28). Assuming that their moving direction changed in response to some signals, most possible attractant is a cAMP molecule, because *D. discoideum* cells have chemotaxis to cAMP (Konijn et al., 1969a;

Koniijn et al., 1969b) as described previously. Cells begin to secret cAMP when starved and drastically change the pattern of gene expressions by using the cAMP molecule as a signal molecule (Gerish et al., 1975; Mann and Firtel, 1987; Mann and Firtel, 1989; Reymond et al., 1995; Iranfar et al., 2003; Loomis, 2014). Not only in aggregation process, cAMP plays important roles at the various stages of development like the morphogenesis and the differentiation (Reymond et al., 1995; Williams, 2010). As a cAMP molecule is biosynthesized from an ATP molecule by adenylyl cyclase in *D. discoideum* (Pitt et al., 1992; Rossomando and Sussman, 1973; Rossomando and Hesla, 1976), cellular ATP concentrations may affect the differentiation via cAMP production in cells. In fact, the observation using DicMaLionG newly revealed that ATP levels were oscillating during aggregation (Fig.29) as same frequent with cAMP pulse (about 6 minutes intervals, Roos et al., 1977; Hashimura et al., 2019), contrary to the previous reports saying that ATP levels were kept constant (Roos et al., 1977). This finding suggested that ATP level actually affects the cAMP production; it might also affect the subsequent differentiation via cAMP signaling. In order to confirm this relationship directly, I generated a new cell strain expressing both ATP indicator (DicMaLionR, Arai et al., 2018) and cAMP indicator (flamindo2, Odaka et al., 2014). Further study using this strain will be desired from now.

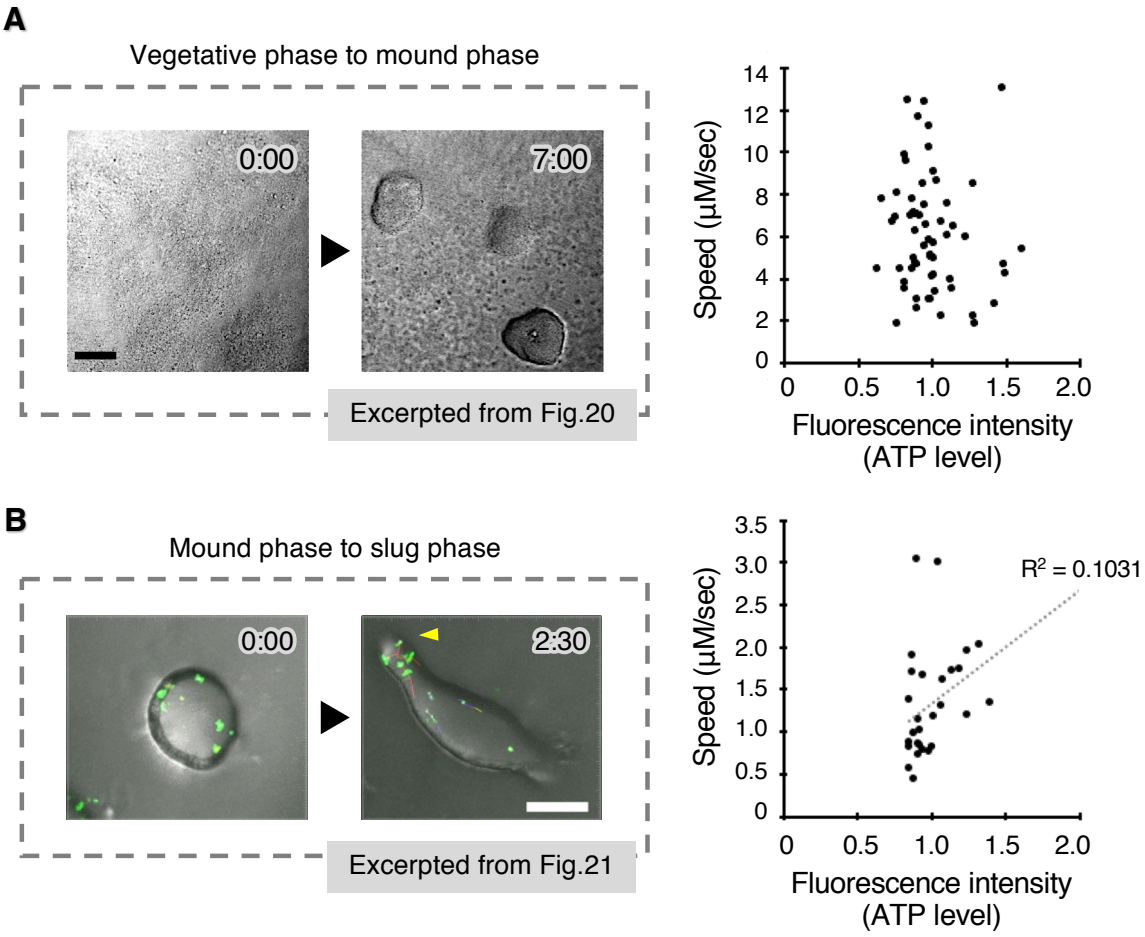

Fig.27 The correlation between cell motilities and ATP levels

(A) Left images showing the aggregation process are excerpted from Fig.20. Cell motility and ATP level (fluorescence intensity of DicMaLionG) were obtained based on this observation result. The horizontal plotted values of right graph are the values obtained by measuring the intensity of each cell and dividing by the mean intensity. The vertical plotted values are the speed obtained by the tracking results of "Imaris" software The number (n) of specimens tested; n = 60.

(B) Left images showing the process of slug formation from a mound are excerpted from Fig.21. Cell motility and ATP level (fluorescence intensity of DicMaLionG) were obtained based on this observation result. Plotted values in the right graph are same with (A); the line indicates the linear regression of the plots. n = 28.

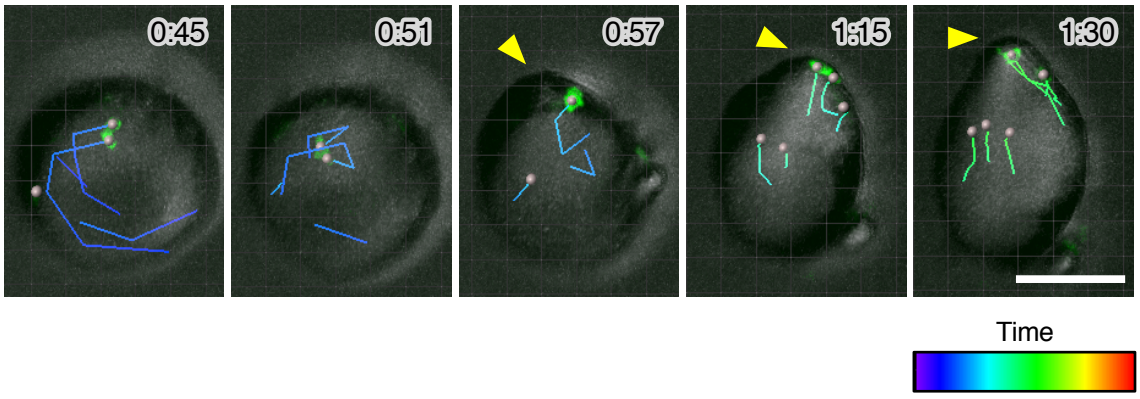

Fig.28 The trajectories of ATP-rich cells during slug formation

Tracking of single cells of interest during development from the mound phase to the slug phase. Images indicate the merged images of bright-field and fluorescence images with trajectories over time. The number in each image indicates time in hours:minutes. Z-stack images were acquired every 3 minutes by Dragonfly200 using a 20× objective lens. The color of trajectories represent the elapsed time as the color scale on the right-bottom. Yellow arrowheads indicate where the anterior prestalk region was formed. Scale bar, 50 μm.

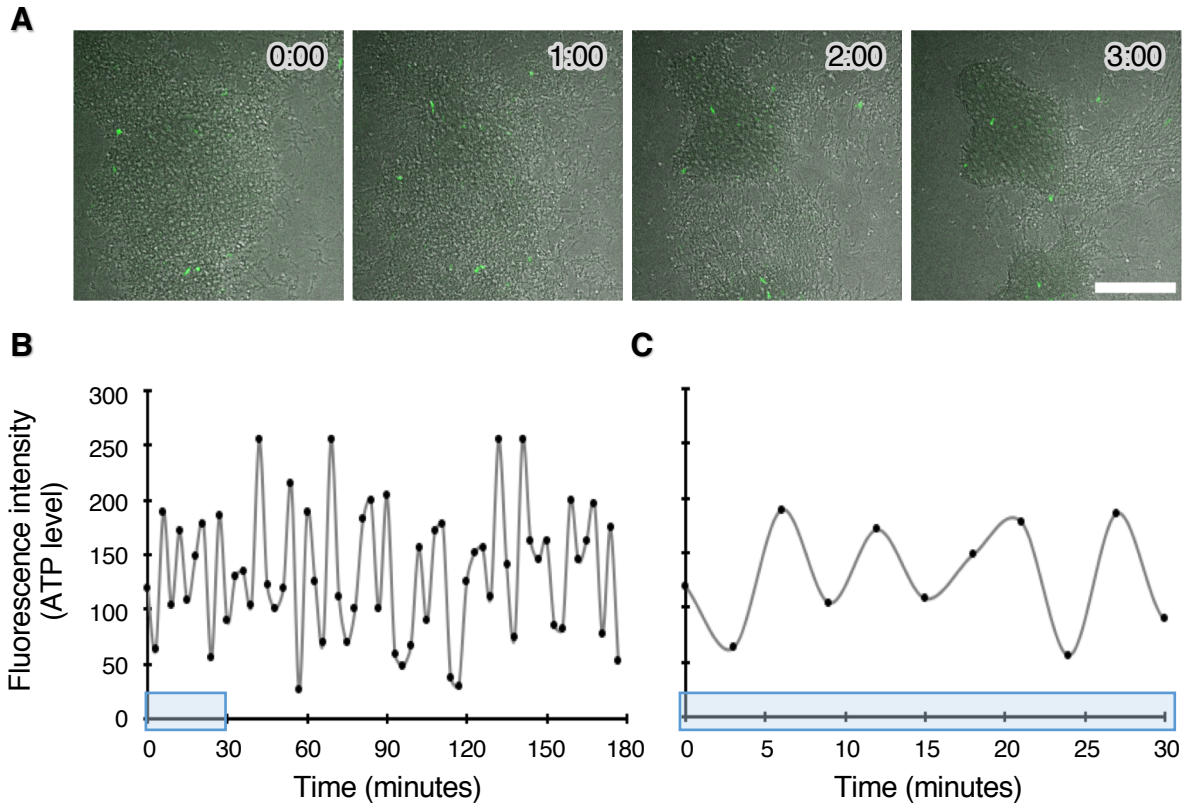

Fig.29 The oscillation of ATP levels during aggregation process

(A) Images to be analyzed, showing the aggregation process of mixed cell population consisting of 1% DicMaLionG cells and wild-type Ax2 cells. Merged images of bright-field and fluorescence images are shown. The number in each image indicates time in hours:minutes. These images were acquired every 3 minutes by Dragonfly200 using a 20× objective lens and projected with the maximum intensity of z-stack images by Fiji. Scale bar, 200 μm.

(B) The change of ATP level (fluorescence intensity of DicMaLionG) of a representative cell shown in (A) over time. Oscillation of ATP level was observed.

(C) Enlarged graph of "0-30 minutes" parts shown by blue box in the graph of (B). Vertical axis is common with graph of (B). During 30 minutes, 4-5 peaks were observed, showing that their oscillation periods are 6-7 minutes.

4-9. The relationship with other factors affecting the differentiation

Finally, I want to discuss the contribution of other factors except for metabolism-related one in stalk-destined and spore-destined cells. As briefly described in chapter 2-3 and 4-1, intracellular calcium concentration and cell cycle stage are known as factors to affect the cell differentiation of *D. discoideum.* Calcium makes an important role to initiate the differentiation (Tanaka et al., 1998), and their concentrations are higher in the anterior prestalk region in a slug (Maeda and Maeda, 1973; Cubbit et al., 1995). Moreover, intracellular calcium concentration at the vegetative phase is known to be related with cell fates tendency; cells with higher calcium concentrations at the vegetative phase differentiate into stalk cells later (Saran et al., 1994; Baskar et al., 2000). So I examined the expression levels of 21 genes which are annotated "up-regulation in presence of calcium" in the "gene description" section of dictyBase. Result showed that 7 out of 21 genes expressed higher in stalk-destined cells and 10 in spore-destined cells; 4 genes were not detected (Table.3). This result was insufficient to suggest that calcium concentration may increase in either of stalk-destined or spore-destined cells.

The relationship between cell cycle stage and differentiation has been also discussed enthusiastically for long time in *D. discoideum* (Katz and Bourguignon, 1974; Zada-Hames and Ashworth, 1978;) and also in human cancer cells (Sherr, 1996). Previous studies about the cell cycle of *D. discoideum* have reported that there is a checkpoint at G2 phase to transfer into the differentiation process from the growth phase (GDT point) and that cell fate of differentiation is determined by the distance from GDT point on the cell cycle when starved (Fig.5) (Ohmori and Maeda, 1987; Maeda et al., 1989). As various genes expressing at GDT point were found in previous works (Maeda, 2005; Maeda, 2011), I first compared the expression levels of those genes based on RNA-seq results, but most of them expressed in neither of stalk-destined and spore-destined cells;

out of 13 genes listed here, 9 were not detected (Table.4). In the level of gene expressions, it remains unclear that those genes expressing at GDT point regulate the differentiation of stalk-destined and spore-destined cells. However, further consideration can be possible by this study revealing the difference of their ATP levels.

ATP level is changed corresponding to the cell cycle stage, that is, ATP level increases near around at M phase (Skog et al., 1982; Marcussen and Larsen, 1996; Sholl-Franco et al., 2010). In order to confirm this fact in *D. discoideum*, I measured the ATP levels in the cell cycle using DicMaLionG. The cell cycle of *D. discoideum* is consist of the following phases: (i) very short M phase (< 15 min), (ii) almost not existed G1 phase, (iii) short S phase (< 30 min) and (ⅳ) G2 phase occupying the majority of cell cycle (Weijer et al., 1984). Based on this duration and the timing of cell division (determined as S phase) which was observed, the phase of each cell was estimated (Fig.30). As reported in other organisms, ATP level was higher at M phase also in *D. discoideum* and then decreased along the proceeding of cell cycle (Fig.30). Taken together with the previous studies about the relationship between cell fates and the distances from GDT point (Fig5 or right-bottom of Fig.30), this result suggests that cells at specific cell cycle stage with high ATP levels differentiate into stalk cells later; it is consistent with the notion demonstrated in this study.

Table.3 RNA-seq analysis results on the calcium-related genes

List of 21 genes annotated as “up-regulation in the presence of calcium” in the "gene description" section in dictyBase. The “FPKM” values indicate the expression levels of each gene provided by NGS service in three RNA-seq measurements. The “Mean ratio” values indicate the mean of the ratios of the expression levels of each gene in the stalk-destined cell to that in the spore-destined cell for three RNA-seq measurements. Color scale on the right are depicted the same rule as that in Fig.8; yellow shows values larger than 2.0; white shows the value of 1; blue shows values less than 0.5. ND indicates “not detected”, in which count values are smaller than 10.

Gene name	Protein name	1st (FPKM)		2nd (FPKM)		3rd (FPKM)		Mean ratio
		stalk-	spore-	stalk-	spore-	stalk-	spore-	
commd1	COMM domain-containing protein 1	7.80	5.88	1.80	2.31	7.09	3.48	1.38
commd10	COMM domain-containing protein 10	29.52	20.45	7.00	7.26	27.37	20.80	1.24
cupJ	ricin B lectin domain-containing protein	18.17	15.00	13.08	10.91	21.44	17.24	1.22
kcnma1	"calcium-activated BK potassium channel, alpha subunit"	1.99	1.65	0.97	0.72	2.27	2.37	1.17
fimA	actin bundling protein	164.51	111.70	169.48	152.79	171.06	193.43	1.16
patA	P-type ATPase	413.42	313.25	487.59	421.95	417.29	600.70	1.06
cnrF	RabGAP/TBC domain-containing protein	14.69	13.98	12.09	11.62	16.13	16.64	1.02
acpA	subunit of heterodimeric actin capping protein cap32/34	569.29	537.42	517.79	499.66	535.96	610.04	0.99
potA	"calcium-activated BK potassium channel, alpha subunit family protein"	1.39	1.28	1.62	1.72	1.75	1.87	0.99
commd7	COMM domain-containing protein 7	28.73	24.96	8.95	11.57	27.33	26.60	0.98
cupD	calcium up-regulated protein	7.05	8.35	2.48	2.20	6.26	11.94	0.83
cupF	calcium up-regulated protein	56.66	64.32	78.70	71.69	72.93	161.98	0.81
cupI	ricin B lectin domain-containing protein	99.36	136.92	548.15	473.33	85.69	181.28	0.79
cupB	calcium up-regulated protein	96.60	137.40	91.96	92.40	114.97	246.12	0.72
cupC	calcium up-regulated protein	56.07	75.52	60.05	59.75	57.85	143.13	0.72
cupH	ricin B lectin domain-containing protein	48.21	68.62	37.08	39.49	62.10	142.48	0.69
cupG	calcium up-regulated protein	56.42	82.97	44.89	47.43	57.08	152.92	0.67
cupA	calcium up-regulated protein	ND	ND	ND	ND	ND	ND	ND
commd2	COMM domain-containing protein 2	ND	ND	ND	ND	ND	ND	ND
commd3	COMM domain-containing protein 3	ND	ND	ND	ND	ND	ND	ND
commd8	COMM domain-containing protein 8	ND	ND	ND	ND	ND	ND	ND

Table.4 RNA-seq analysis results on the cell cycle-related genes

List of 13 genes related to *D. discoideum* development reported in previous studies (Maeda, 2005; Maeda, 2011). The "FPKM" values indicate the expression levels of each gene provided by NGS service in three RNA-seq measurements. The "Mean ratio" values indicate the mean of the ratios of the expression levels of each gene in the stalk-destined cell to that in the spore-destined cell for three RNA-seq measurements. ND indicates "not detected", in which count values are smaller than 10.

Gene name	Protein name	1st (FPKM)		2nd (FPKM)		3rd (FPKM)		Mean ratio
		stalk-	spore-	stalk-	spore-	stalk-	spore-	
carA-1	cAMP receptor 1	ND	ND	ND	ND	ND	ND	ND
carA-2	cAMP receptor 2	ND	ND	ND	ND	ND	ND	ND
mrps4	ribosomal protein S4, mitochondrial	ND	ND	ND	ND	ND	ND	ND
dia2	hypothetical protein DDB_G0291253	13.55	59.66	12.65	13.55	24.71	30.91	0.65
dia1	hypothetical protein DDB_G0285431	0.88	1.00	0.74	0.71	1.09	1.07	0.98
cafA	calfumirin-1	13.79	15.13	17.00	5.88	25.96	11.79	2.00
dscA-1	discoidin I, alpha chain	ND	ND	ND	ND	ND	ND	ND
dscA-2	discoidin I, alpha chain	ND	ND	ND	ND	ND	ND	ND
dscC-1	discoidin I, beta/gamma chain	ND	ND	ND	ND	ND	ND	ND
dscC-2	discoidin I, beta/gamma chain	ND	ND	ND	ND	ND	ND	ND
dscD-1	discoidin I, delta chain	ND	ND	ND	ND	ND	ND	ND
dscD-2	discoidin I, delta chain	ND	ND	ND	ND	ND	ND	ND
nxnA	annexin VII	1164.16	1073.03	1528.27	1418.91	1307.47	1607.23	0.99

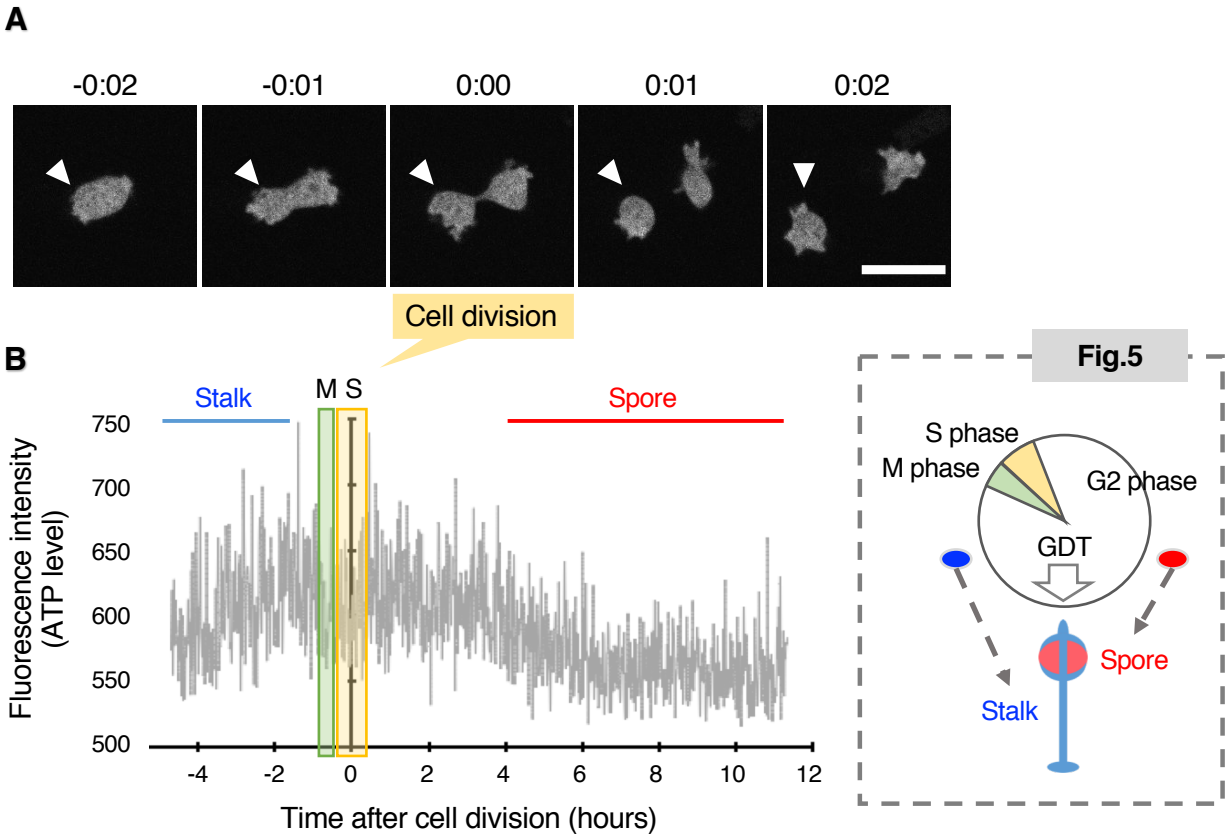

Fig.30 The changes of ATP levels along the cell cycle

(A) Representative images of cell division; this is a part of long observation against cells cultured in HL5 medium. The number above each image indicates time in hours:minutes with setting the timing of cell division as 0:00. These images were acquired every 1 minute by Dragonfly200 using a 60× oil immersion objective lens. White arrowheads indicate the target cells to be analyzed ATP level in (C). Scale bar, 20 μm.

(B) The change of ATP level (fluorescence intensity of DicMaLionG) over time of a cell indicated by white arrowheads in (A). Their cell cycle phase shown here were determined based on the timing of cell division. Expected future cell fate from previous studies shown on the right (referred from Fig.5) are indicated by blue (stalk) and red (spore).

5. Discussion

5-1. Metabolic activity and differentiation in various organisms

The regulatory mechanism to determine the cell fates is a fundamental question in many organisms including humans, and also in cellular slime molds. For long time, we cannot identify the stalk and spore progenitor cells until the slug phase when their spatial positions in a slug were determined. Therefore, various differences of the characteristic of prestalk and prespore cells in a slug have been reported and discussed so far in order to reveal the mechanism of cell fate determination. Following factors are examples of their characteristic: gene expression levels, motility, sensitivity of some attractants, and so on (Maeda and Maeda, 1973; Traynor et al., 1992; Abe et al., 1994; Cubbit et al., 1995; Early et al., 1995; Rietdorf et al., 1996; Maeda et al, 2003; Fujimori et al., 2019). Cell fate determination of those cells in a slug is already completed, and it was difficult to know the differentiation-inducing factors working before the fate determination.

However, recent study enabled us to predict the cell fates at the vegetative phase by identifying *omt12* gene as a marker of future cell fates (Kuwana et al., 2016). In this study, I investigated the characteristic of stalk-destined and spore-destined cells at the vegetative phase by applying this advantage, showing that ATP levels are higher in stalk-destined cells probably due to the multiplication of the activation of metabolism-related genes. In supporting this notion, mitochondrial activity has been proposed as an important factor in the differentiation of cellular slime molds (Matsuyama and Maeda, 1995; Inazu et al.,1999; Chida et al., 2004; Kimura et al., 2010). Since mitochondria are intracellular organelle that produce ATP (Cooper, 2000), these previous studies support my hypothesis that cellular ATP levels influence the cell fate in differentiation.

As similar with cellular slime molds, recent studies have demonstrated the relationship between intracellular metabolic states and differentiation fates in various living organisms, including mice and humans (Cho et al., 2006; Simsek et al., 2010; Tan

et al., 2011; Takubo et al., 2013; Shiraki et al., 2014; Buck et al., 2016; Berger et al., 2016; Yang et al., 2016; Schell et al., 2017; Lees et al., 2017; Rodríguez-Colman et al., 2017). For example, it has been shown that upregulation of metabolism-related genes, especially glycolysis-related genes, promoted the activation of immune B cells during their early stages of differentiation (Dufort et al., 2007; Aronov and Tirosh, 2016; Price et al., 2018). Furthermore, another study demonstrated the increased mitochondrial biogenesis and ATP production during the early differentiation of human embryonic stem cells (Cho et al., 2006). Interestingly, some of these studies argue that the ratio of glycolysis and oxidative phosphorylation usage (Takubo et al., 2013; Buck et al., 2016) and amounts of the metabolites produced in each pathway (Khacho et al., 2016) have an effect on cell fates at the growth/differentiation transition. Furthermore, in cancer and stem cell as well, it has been reported that the metabolism shift between glycolysis and oxidative phosphorylation has an effect on their fates at the growth/differentiation transition (Matoba et al., 2006; Hsu and Sabatini, 2008; Meylan et al., 2009; Koppenol, 2011;). Although the significance of usage of these pathways has been debated, it has possibility that ATP as a final product of these pathways is an actual effector in other organisms.

5-2. The mechanism by an ATP affecting the cell fates

However, it remains unknown how ATP levels affect the cell fates. This study showed that cell motility do not have the correlation with ATP level, whereas cAMP sensitivity appears to be related with ATP perhaps via the activation of cAMP production and signaling by abundant ATP molecules; but it remains unclear. On the other hands, the fact that ATP, a universal molecule, is involved in differentiation suggests that such ATP-dependent regulatory mechanism is commonly used in other living organisms. Assuming that ATP acts as an actual effector in other organisms, there expected to be something

general mechanism in addition to the specific cues in cellular slime molds. One possibility is that activation of ATP production processes, or high ATP levels as a result, could affect gene expression in the nucleus. This idea was supported by the reports that ROS generated through ATP production switch the gene expression patterns to determine the cell fates of the differentiation of immune cells (Buck et al., 2016) and neuronal stem cells (Khacho et al., 2016). Another possibility is that ATP acts to bring about drastic changes in cellular structures, including changes in mitochondrial structures that drive cell differentiation as reported previously (Matsuyama and Maeda, 1995; Buck et al., 2016; Khacho et al., 2016). In either case, the targets affected by ATP is commonly existed in various eukaryotes.

Moreover, the result in this study suggested the possibility that cell fates are regulated by relative values of cellular ATP concentrations among cells, not by the absolute values. It suggested that cells have some mechanism to sense the intracellular condition each other. In this perspective, mitochondria can be an influential candidate to be affected by ATP. Mitochondria acts as a sensor of intercellular and extracellular condition, as it functions in multiple important cellular processes like autophagy or signaling pathway (Rambold and Lippincott-Schwartz, 2011; Shadel and Horvath, 2015; Akbari et al., 2019). In addition, the effect to surrounding cells was also reported, showing that defect in mitochondrial function affects adjacent cells via the expression of secreted proteins (Ohsawa et al., 2012). These facts support the relative determination mechanism by the changes of mitochondrial structure or function via the changes of ATP levels.

5-3. Differentiation of ATP-rich cells into stalk cells to be removed

Abundant ATP molecules as a result of activation of metabolism appears to be good signature for cells as they have a lot of energy. In *Dictyostelium*, approximately 20% of the total cells differentiate into stalk cells and are removed by apoptosis thereafter,

whereas the remaining cells propagate to offspring as spores (Bonner and Dodd, 1962; Hayashi and Takeuchi, 1976; Hashimoto et al., 1988). However, results in this study demonstrate that ATP-rich cells preferentially differentiate into stalk cells for removal, and cells with low ATP levels are selected for spores to survive; it raises the question why ATP-rich cells are destined to be removed.

A possible answer for this question is that cells with high ATP levels are likely to maintain high mitochondrial activities, and hence, mitochondrial DNA in these cells can be more damaged by ROS produced by the higher mitochondrial activities. Therefore, it is tempting to speculate that ATP-rich cells, which may carry damaged mitochondrial DNA, are removed as stalk cells. This hypothesis is supported by the evidence showing that cells carrying damaged mitochondrial DNA tend to differentiate into stalk cells (Chida et al., 2004).

5-4. The relationship between ATP levels and other differentiation factors

As described in previous chapter, intracellular calcium concentration, cell cycle stage, and metabolism have been proposed as possible cell fate determinants in *Dictyostelium*. Previous studies have reported that intracellular calcium concentration is involved in differentiation (Maeda and Maeda, 1973; Saran et al., 1994; Cubbit et al., 1995; Baskar et al., 2000), and that cell cycle stage plays a role in the process of differentiation (Katz and Bourguignon, 1974; Zada-Hames and Ashworth, 1978; Maeda et al., 1989; Maeda, 2005; Maeda, 2011). It has been proposed that cell cycle stage when staved determine the direction of differentiation and that several genes are known to function at the GDT point (Maeda, 2005; Maeda, 2011). Moreover, the contribution to differentiation of metabolism, mitochondrial activity and glucose concentration in culture medium, was also reported in previous studies (Leach et al., 1973; Tasaka and Takeuchi, 1981; Matsuyama and Maeda,

1995; Inazu et al.,1999; Chida et al., 2004; Maeda, 2005; Kimura et al., 2010). These study support an idea obtained in this study that cellular ATP levels influence the cell fate determination in *Dictyostelium* differentiation.

On the other hands, the increasing of calcium concentration in stalk-destined or spore-destined cells was not suggested by RNA-seq results in this study. However, an intracellular calcium ion is stored in endoplasmic reticulum (ER) (Soboloff et al., 2012) and mitochondria (Berridge et al., 2003; Stefani et al., 2011) and the intracellular concentration of calcium is regulated by influx from those organelles. Therefore, calcium concentration can be related to the mitochondrial activity and ATP concentration. To confirm it directly, calcium concentration should be observed in ATP-rich and ATP-poor cell in future. Anyway, the contribution of intracellular calcium concentration to cell differentiation is uncertain in this study so far; further investigation is expected.

In contrast, the relationship between ATP level and cell cycle stage was revealed in this study. ATP level of *Dictyostelium* cells changed along the proceeding of cell cycle with a similar pattern as reported about other organisms in previous studies (Skog et al., 1982; Marcussen and Larsen, 1996; Sholl-Franco et al., 2010). ATP level was higher in cells around at M phase, a phase reported the differentiation into stalk cells (Ohmori and Maeda, 1987; Maeda et al., 1989). Previous studies also reported about the relationship between calcium level and cell cycle stage, that is, calcium level is relatively higher in cells at S phase to early G2 phase, whereas cells at mid to late G2 phase have relatively lower calcium levels (Azhar et al., 2001). It consists with notion about cell cycle stage that cells at S phase, M phase, or early G2 phase have tendency to differentiate into stalk cells. These facts suggest that there is a common mechanism in cell fate determination by the factors reported as determinants.

6. Conclusion

In conclusion, this study proposed that an ATP influence the cell fate determination in *D. discoideum* differentiation. The variation of ATP levels among cells might be derived from the levels of mitochondrial activity. High mitochondrial activity resulting high ATP level can cause the damage to mitochondrial DNA via the ROS generation. Such cellular damages possibly make ATP-rich cells differentiate into stalk cells, the dead cells to be removed for supporting spores. In addition, several results suggested the possibility that ATP levels of *D. discoideum* have a relationship with other determinant factors reported in previous studies: intracellular calcium concentration and cell cycle stage. I expect to be able to elucidate the differentiation mechanism by considering the facts which have been reported in those studies.

Recently, the differentiation mechanism regulated by metabolic activity have been discussed also in other living organisms enthusiastically. Although the underlying mechanism remains to be elucidated, same notion obtained in this study may be conserved among a wide range of organisms as ATP is widely conserved among organisms.

7. Reference

1. Abe, T., Early, A., Siegert, F., Weijer, C., and Williams, J. (1994). Patterns of cell movement within the *Dictyostelium* slug revealed by cell type-specific, surface labeling of living cells. *Cell* **77**, 687-699. https://doi.org/10.1016/0092-8674(94)90053-1

2. Akbari, M., Kirkwood, T.B.L., and Bohr, V.A. (2019). Mitochondria in the signaling pathways that control longevity and health span. *Ageing Res. Rev.* **54**, 100940. https://doi.org/10.1016/j.arr.2019.100940

3. Alvarado, A.S., and Yamanaka, S. (2014). Rethinking Differentiation: Stem Cells, Regeneration, and Plasticity. *Cell* **157**, 110-119. https://doi.org/10.1016/j.cell.2014.02.041

4. Arai, S., Kriszt, R., Harada, K., Looi, L.S., Matsuda, S., Wongso, D., Suo, S., Ishiura, S., Tseng, Y.H., Raghunath, M., Ito, T., Tsuboi, T., and Kitaguchi, T. (2018). RGB-Color Intensiometric Indicators to Visualize Spatiotemporal Dynamics of ATP in Single Cells. *Angew. Chem. Int. Ed. Engl.* **57**, 10873-10878. https://doi.org/10.1002/anie.201804304

5. Aronov, M., and Tirosh, B. (2016). Metabolic Control of Plasma Cell Differentiation-What We Know and What We Don't Know. *J. Clin. Immunol. 36 Suppl* **1**, 12-17. https://doi.org/10.1007/s10875-016-0246-9

6. Avior, Y., Sagi, I., and Benvenisty, N. (2016). Pluripotent stem cells in disease modelling and drug discovery. *Nat. Rev. Mol. Cell Biol.* **17**, 170-182. https://doi.org/10.1038/nrm.2015.27

7. Azhar, M., Kennady, P.K., Pande, G., Espiritu, M., Holloman, W., Brazill, D., Gomer, R.H., and Nanjundiah, V. (2001). Cell cycle phase, cellular Ca^{2+} and development in *Dictyostelium discoideum*. *Int. J. Dev. Biol.* **45**, 405-414.

8. Baskar, R., Chhabra, P., Mascarenhas, P., and Nanjundiah, V. (2000). A cell type-specific effect of calcium on pattern formation and differentiation in *Dictyostelium discoideum*. *Int. J. Dev. Biol.* **44**, 491-498.

9. Berger, E., Rath, E., Yuan, D., Waldschmitt, N., Khaloian, S., Allgäuer, M.,

Staszewski, O., Lobner, E.M., Schöttl, T., Giesbertz, P., Coleman, O.I., Prinz, M., Weber, A., Gerhard, M., Klingenspor, M., Janssen, K.P., Heikenwalder, M., and Haller, D. (2016). Mitochondrial function controls intestinal epithelial stemness and proliferation. *Nat. Commun.* **7**, 13171. https://doi.org/10.1038/ncomms13171

10. Berridge, J.M., Bootman, M.D., and Roderick, H.L. (2003). Calcium signalling: dynamics, homeostasis and remodelling. *Nat. Rev. Mol. Cell Biol*. **4**, 517-529. https://doi.org/10.1038/nrm1155

11. Bonner, J.T., and Dodd, M.R. (1962). Aggregation territories in the cellular slime molds. *Biological Bulletin* **122**, 13-24. https://doi.org/10.2307/1539317

12. Buck, M.D., O'Sullivan, D., Klein Geltink, R.I., Curtis, J.D., Chang, C.H., Sanin, D.E., Qiu, J., Kretz, O., Braas, D., van der Windt, G.J., Chen, Q., Huang, S. C., O'Neill, C.M., Edelson, B.T., Pearce, E.J., Sesaki, H., Huber, T.B., Rambold, A.S., and Pearce, E.L. (2016). Mitochondrial dynamics controls T cell fate through metabolic programming. *Cell* **166**, 63-76. https://doi.org/10.1016/j.cell.2016.05.035

13. Castanon, I., and González-Gaitán, M. (2011). Integrating levels of complexity: a trend in developmental biology. *Curr. Opin. Cell Biol.* **23**, 647-649. https://doi.org/10.1016/j.ceb.2011.10.003

14. Chagastelles, P.C., and Nardi, N.B. (2011). Biology of stem cells: an overview. *Kidney Inter. Suppl.* **1**, 63-67. https://doi.org/10.1038/kisup.2011.15

15. Chappell, J.B., and Greville, G.D. (1961). Effects of oligomycin on respiration and swelling of isolated liver mitochondria. *Nature* **190**, 502-504. https://doi.org/10.1038/190502a0

16. Chattwood, A., and Thompson, C.R.L. (2011). Non-genetic heterogeneity and cell fate choice in *Dictyostelium discoideum. Dev. Growth Differ.* **53**, 558-566. https://doi.org/10.1111/j.1440-169X.2011.01270.x.

17. Chida, J., Yamaguchi, H., Amagai, A., and Maeda, Y. (2004). The necessity of mitochondrial genome DNA for normal development of *Dictyostelium* cells. *J. Cell Sci.* **117**, 3141-3152. https://doi.org/10.1242/jcs.01140

18. Cho, Y.M., Kwon, S., Pak, Y.K., Seol, H.W., Choi, Y.M., Park, D.J., Park, K.S., and Lee, H.K. (2006). Dynamic changes in mitochondrial biogenesis and antioxidant enzymes during the spontaneous differentiation of human embryonic stem cells. *Biochem. Biophys. Res. Commun.* **348**, 1472-1478. https://doi.org/10.1016/j.bbrc.2006.08.020

19. Cooper, G.M. (2000). Bioenergetics and metabolism. In *The Cell, A Molecular Approach, 2nd edition.* (Sinauer Associates Sunderland (MA)), ISBN-10: 0-87893-106-6, pp. 387-420.

20. Cubbit, A.B., Firtel, R.A., Fischer, G., Jaffe, L.F., and Miller, A.L. (1995). Patterns of free calcium in multicellular stages of *Dictyostelium* expressing jellyfish apoaequorin. *Development* **121**, 2291-2301.

21. Cunningham, C.C., and George, D.T. (1974). The relationship between the bovine heart mitochondrial adenosine triphosphatase, lipophilic compounds, and oligomycin. *J. Biol. Chem.* **250**, 2036-2044.

22. Dufort, F.J., Bleiman, B.F., Gumina, M.R., Blair, D., Wagner, D.J., Roberts, M.F., Abu-Amer, Y., and Chiles, T.C. (2007). Cutting edge: IL-4-mediated protection of primary B lymphocytes from apoptosis via Stat6-dependent regulation of glycolytic metabolism. *J. Immunol.* **179**, 4953-4957. https://doi.org/10.4049/jimmunol.179.8.4953

23. Early, A.E., Williams, J.G., Meyer, H.E., Por, S.B., Smith, E., Williams, K.L., and Gooley, A.A. (1988). Structural characterization of *Dictyostelium discoideum* prespore-specific gene *D19* and of its product, cell surface glycoprotein PsA. *Mol. Cell Biol*. **8**, 3458-3466. https://doi.org/10.1128/MCB.8.8.3458

24. Early, A.E, Abe, T., and Williams, J.G. (1995). Evidence for positional differentiation of prestalk cells and for a morphogenetic gradient in *dictyostelium*. *Cell* **83**, 91-99. https://doi.org/10.1016/0092-8674(95)90237-6

25. Fujimori, T., Nakajima, A., Shimada, N., and Sawai, S. (2019). Tissue self-organization based on collective cell migration by contact activation of locomotion and chemotaxis. *Proc. Natl. Acad. Sci. USA* **116**, 4291-4296. https://doi.org/10.1073/

pnas.1815063116

26. Gerish, G., Fromm, H., Huesgen, A., and Wick, U. (1975). Control of cell-contact sites by cyclic AMP pulses in differentiating *Dictyostelium* cells. *Nature* **255**, 547-549. https://doi.org/10.1038/255547a0

27. Geschwind, J.-F.H., Ko, Y.H., Torbenson, M.S., Magee, C., and Pedersen, P.L. (2002). Novel Therapy for Liver Cancer. *Cancer Res.* **62**, 3909-3913.

28. Ghosh, R., Chhabra, A., Phatale, P.A., Samrat, S.K., Sharma, J., Gosain, A., Mohanty, D., Saran, S., and Gokhale, R.S. (2008). Dissecting the functional role of polyketide synthases in *Dictyostelium discoideum*; biosynthesis of the differentiation regulating factor 4-methyl-5-pentylbenzene-1, 3-diol. *J. Biol. Chem.* **283**, 11348-11354. https://doi.org/10.1074/jbc.M709588200

29. Grant, W.N., Welker, D.L., and Williams, K.L. (1985). A polymorphic, prespore-specific cell surface glycoprotein is present in the extracellular matrix of *Dictyostelium discoideum*. *Mol. Cell Biol*. **5**, 2559-2566. https://doi.org/10.1128/MCB.5.10.2559

30. Hashimoto, Y., Nakamura, R., Muroyama, T., and Yamada, T. (1988). Studies on tiny fruiting bodies of the cellular slime mold, *Dictyostelium discoideum*. *Cytologia* **53**, 337-340. https://doi.org/10.1508/cytologia.53.337

31. Hashimura, H., Morimoto., Y.V., Yasui, M., and Ueda., M. (2019). Collective cell migration of *Dictyostelium* without cAMP oscillations at multicellular stages. *Commun Biol.* **2**, 34. https://doi.org/10.1038/s42003-018-0273-6

32. Hayashi, M., and Takeuchi, I. (1976). Quantitative studies on cell differentiation during morphogenesis of the cellular slime mold *Dictyostelium discoideum*. *Dev. Biol.* **50**, 302-309. https://doi.org/10.1016/0012-1606(76)90153-6

33. Hsu, P.P., and Sabatini, D.M. (2008). Cancer cell metabolism: Warburg and beyond. *Cell* **134**, 703-707. https://doi.org/10.1016/j.cell.2008.08.021

34. Iijima, M. and Devreotes, P. (2002). Tumor suppressor PTEN mediates sensing of chemoattractant gradients. *Cell* **109**, 599-610. https://doi.org/10.1016/s0092-8674

(02)00745-6

35. Imamura, H., Nhat, K.P., Togawa, H., Saito, K., Iino, R., Kato-Yamada, Y., Nagai, T., and Noji, H. (2009). Visualization of ATP levels inside single living cells with fluorescence resonance energy transfer-based genetically encoded indicators. *Proc. Natl. Acad. Sci. USA* **106**, 15651-15656. https://doi.org/10.1073/pnas.0904764106

36. Inazu, Y., Chae, S.C., and Maeda, Y. (1999). Transient expression of a mitochondrial gene cluster including *rps4* is essential for the phase-shift of *Dictyostelium* cells from growth to differentiation. *Dev. Genet.* **25**, 339-352. https://doi.org/10.1002/(SICI)1520-6408(1999)25:4<339::AID-DVG8>3.0.CO;2-3

37. Iranfar, N., Fuller, D., and Loomis, W.F. (2003). Genome-wide expression analyses of gene regulation during early development of *Dictyostelium discoideum. Eukaryot. cell* **2**, 664-670. https://doi.org/10.1128/EC.2.4.664-670.2003

38. Ito, K., and Suda, T. (2014). Metabolic requirements for the maintenance of self-renewing stem cells. *Nat. Rev. Mol. Cell Biol.* **15**, 243-256. https://doi.org/10.1038/nrm3772

39. Kamimura, Y., Miyanaga, Y., and Ueda, M. (2016). Heterotrimeric G-protein shuttling via Gip1 extends the dynamic range of eukaryotic chemotaxis. *Proc. Natl. Acad. Sci. USA* **113**, 4356-4361. https://doi.org/10.1073/pnas.1516767113

40. Katz, E.R., and Bourguignon, L.Y.W. (1974). The cell cycle and its relationship to aggregation in the cellular slime mold, *Dictyostelium discoideum*. *Dev. Biol.* **36**, 82-87. https://doi.org/10.1016/j.stem.2016.04.015

41. Khacho, M., Clark, A., Svoboda, D.S., Azzi, J., MacLaurin, J.G., Meghaizel, C., Sesaki, H., Lagace, D.C., Germain, M., Harper, M.E., Park, D.S., and Slack, R.S. (2016). Mitochondrial Dynamics Impacts Stem Cell Identity and Fate Decisions by Regulating a Nuclear Transcriptional Program. *Cell Stem Cell* **19**, 232-247. https://doi.org/10.1016/j.stem.2016.04.015

42. Kim S.-B., and Berdanier, C.D. (1999). Oligomycin sensitivity of mitochondrial F_1F_0-ATPase in diabetes-prone BHE/Cdb rats. *Am. J. Physiol. Endocrinol. Metab.* **277**,

E702-707. https://doi.org/10.1152/ajpendo

43. Kimura, K., Kuwayama, H., Amagai, A., and Maeda, Y. (2010). Developmental significance of cyanide-resistant respiration under stressed conditions: experiments in *Dictyostelium* cells. *Dev. Growth Differ.* **252**, 645-656. https://doi.org/10.1111/j.1440-169X.2010.01200.x

44. Ko, Y.-H., Pedersen, P.L., and Geschwind, J.F. (2001). Glucose catabolism in the rabbit X2 tumor model for liver cancer: characterization and targeting hexokinase. *Cancer Letters* **173**, 83-91. https://doi.org/10.1016/s0304-3835(01)00667-x

45. Konijn, T.M., van de Meene, J.G., Chang, Y.Y., Barkley, D.S., and Bonner, J.T. (1969a). Identification of adenosine-3',5'-monophosphate as the bacterial attractant for myxamoebae of *Dictyostelium discoideum*. *J. Bacteriol*. **99**, 510-512.

46. Konijn, T.M., Chang, Y.Y., and Bonner, J.T. (1969b). Synthesis of cyclic AMP in *Dictyostelium discoideum* and *Polysphondylium pallidum*. *Nature* **224**, 1211-1212. https://doi.org/10.1038/2241211a0

47. Koppenol, W.H., Bounds, P.L., and Dang, C.V. (2011). Otto Warburg's contributions to current concepts of cancer metabolism. *Nat. Rev. Cancer* **11**, 325-337. https://doi.org/10.1038/nrc3038

48. Kuwana, S., Senoo, H., Sawai, S., and Fukuzawa, M. (2016). A novel, lineage-primed prestalk cell subtype involved in the morphogenesis of *D. discoideum*. *Dev. Biol.* **416**, 286-299. https://doi.org/10.1016/j.ydbio.2016.06.032

49. Leach, C.K., Ashworth, J.M., and Garrod, D.R. (1973). Cell sorting out during the differentiation of mixtures of metabolically distinct populations of *Dictyostelium discoideum. Development* **29**, 647–661.

50. Lees, J.G., Gardner, D.K., and Harvey, A.J. (2017). Pluripotent Stem Cell Metabolism and Mitochondria: Beyond ATP. *Stem Cells* 2874283. https://doi.org/10.1155/2017/2874283

51. Loomis, W.F. (2014). Cell signaling during development of *Dictyostelium*. *Dev. Biol.* **391**, 1-16. https://doi.org/10.1016/j.ydbio.2014.04.001

52. Maeda, M., Sakamoto, H., Iranfar, N., Fuller, D., Maruo, T., Ogihara, S., Morio, T., Urushihara, H., Tanaka, Y., and Loomis, W.F. (2003). Changing patterns of gene expression in *Dictyostelium* prestalk cell subtypes recognized by in situ hybridization with genes from microarray analyses. *Eukaryot. Cell* **2**, 627-637. https://doi.org/10.1128/EC.2.3.627-637.2003

53. Maeda, Y., and Maeda, M. (1973). The calcium content of the cellular slime mold, *Dictyostelium discoideum,* during development and differentiation. *Exp. Cell Res.* **82**, 125–130. https://doi.org/10.1016/0014-4827(73)90253-X

54. Maeda, Y., Ohmori, T., Abe, T., Abe, F., and Amagai, A. (1989). Transition of starving *Dictyostelium* cells to differentiation phase at a particular position of the cell cycle. *Differentiation* **41**, 169-175. https://doi.org/10.1111/j.1432-0436.1989.tb00744.x

55. Maeda, Y., Inouye, K., and Takeuchi, I. (1997). *A Model System for Cell and Developmental Biology* (Universal Academy Press, Inc., Tokyo, Japan; Frontiers Science series No.21), pp. 3-6.

56. Maeda, Y. (2005). Regulation of growth and differentiation in *Dictyostelium*. *Int. Rev. Cytol.* **244**, 287–332. https://doi.org/10.1016/S0074-7696(05)44007-3

57. Maeda, Y. (2011). Cell-cycle checkpoint for transition from cell division to differentiation. *Develop. Growth Differ.* **53**, 463-481. https://doi.org/10.1111/j.1440-169X.2011.01264.x

58. Mann, S.K., and Firtel, R.A. (1987). Cyclic AMP regulation of early gene expression in *Dictyostelium discoideum*: mediation via the cell surface cyclic AMP receptor. *Mol. Cell Biol.* **7**, 458-469. https://doi.org/10.1128/MCB.7.1.458

59. Mann, S.K., and Firtel, R.A. (1989). Two-phase regulatory pathway controls cAMP receptor-mediated expression of early genes in *Dictyostelium. Proc. Natl. Acad. Sci. USA* **86**, 1924-1928. https://doi.org/10.1073/pnas.86.6.1924

60. Marcussen, M., and Larsen, P.J. (1996). Cell cycle-dependent regulation of cellular ATP concentration, and depolymerization of the interphase microtubular network induced by elevated cellular ATP concentration in whole fibroblasts. *Cell motil.*

cytoskelet. **35**, 94-99. https://doi.org/10.1002/(SICI)1097-0169(1996)35:2<94::AID-CM2>3.0.CO;2-I

61. Matoba, S., Kang, J.G., Patino, W.D., Wragg, A., Boehm, M., Gavrilova, O., Hurley, P.J., Bunz, F., and Hwang, P.M. (2006). P53 regulates mitochondrial respiration. *Science* **312**, 1650-1653. https://doi.org/10.1126/science.1126863

62. Matsuyama, S.I., and Maeda, Y. (1995). Involvement of cyanide-resistant respiration in cell-type proportioning during *Dictyostelium* development. *Dev. Biol.* **172**, 182-191. https://doi.org/10.1006/dbio.1995.0014

63. McRobbie, S.J., Tilly, R., Blight, K., Ceccarelli, A., and Williams, J.G. (1988). Identification and localization of proteins encoded by two DIF-inducible genes of *Dictyostelium*. *Dev. Biol*. **125**, 59-63. https://doi.org/10.1016/0012-1606(88)90058-9

64. Meylan, E., Dooley, A.L., Feldser, D.M., Shen, L., Turk, E., Ouyang, C., and Jacks, T. (2009). Requirement for NF-kappaB signaling in a mouse model of lung adenocarcinoma. *Nature* **462**, 104-107. https://doi.org/10.1038/nature08462

65. Morrissey, J.H., Devine, K.M., and Loomis, W.F. (1984). The timing of cell-type-specific differentiation in *Dictyostelium discoideum*. *Dev. Biol*. **103**, 414-424. https://doi.org/10.1016/0012-1606(84)90329-4

66. Narita, T.B., Koide, K., Morita, N., and Saito, T. (2011). *Dictyostelium* hybrid polyketide synthase, SteelyA, produces 4-methyl-5-pentylbenzene-1,3-diol and induces spore maturation. *FEMS Microbio. Letters* **319**, 82-87. https://doi.org/10.1111/j.1574-6968.2011.02273.x

67. Narita, T.B., Chen, Z.H., Schaap, P., and Saito, T. (2014). The hybrid type polyketide synthase steelyA is required for cAMP signalling in early *Dictyostelium* development. *PLoS ONE* **9**, e106634. https://doi.org/10.1371/journal.pone.0106634

68. Odaka, H., Arai, S., Inoue, T., and Kitaguchi T. (2014). Genetically-encoded yellow fluorescent cAMP indicator with an expanded dynamic range for dual-color imaging. *PLoS ONE* **9**, e100252. https://doi.org/10.1371/journal.pone.0100252

69. Ohmori, T., and Maeda, Y. (1987). The developmental fate of *Dictyostelium*

discoideum cells depends greatly on the cell-cycle position at the onset of starvation. *Cell Differ*. **22**, 11-18. https://doi.org/10.1016/0045-6039(87)90409-X

70. Ohsawa, S., Sato, Y., Enomoto, M., Nakamura, M., Betsumiya, A., and Igaki, T. (2012). Mitochondrial defect drives non-autonomous tumour progression through Hippo signalling in *Drosophila*. *Nature* **490**, 547-551. https://doi.org/10.1038/nature11452

71. Pitt, G.S., Milona, N., Borleis, J., Lin, K.C., Reed, R.R., and Devreotes P.N. (1992). Structurally distinct and stage-specific adenylyl cyclase genes play different roles in *dictyostelium* development. *Cell* **69**, 305-315. https://doi.org/10.1016/0092-8674(92)90411-5

72. Price, M.J., Patterson, D.G., Scharer, C.D., and Boss, J.M. (2018). Progressive Upregulation of Oxidative Metabolism Facilitates Plasmablast Differentiation to a T-Independent Antigen. *Cell Rep.* **23**, 3152-3159. https://doi.org/10.1016/j.celrep.2018.05.053

73. Rambold, A.M., and Lippincott-Schwartz, J. (2011). Mechanisms of mitochondria and autophagy crosstalk. *Cell Cycle* **10**, 4032-4038. https://doi.org/10.4161/cc.10.23.18384

74. Reymond, C.D., Schaap, P., Veron, M., and Williams, J.G. (1995). Dual role of cAMP during *Dictyostelium* development. *Experientia* **51**, 1166–1174. https://doi.org/10.1007/BF01944734

75. Rietdorf, J., Siegert, F., and Weijer, C.J. (1996). Analysis of optical density wave propagation and cell movement during mound formation in *Dictyostelium discoideum*. *Dev. Biol.* **177**, 427-438. https://doi.org/10.1006/dbio.1996.0175

76. Rodríguez-Colman, M.J., Schewe, M., Meerlo, M., Stigter, E., Gerrits, J., Pras-Raves, M., Sacchetti, A., Hornsveld, M., Oost, K.C., Snippert, H.J., Verhoeven-Duif, N., Fodde, R., and Burgering, B.M. (2017). Interplay between metabolic identities in the intestinal crypt supports stem cell function. *Nature* **543**, 424-427. https://doi.org/10.1038/nature21673

77. Roos, W., Scheidegger, C., and Gerisch, G. (1977). Adenylate cyclase activity

oscillations as signals for cell aggregation in *Dictyostelium discoideum*. *Nature* **266**, 259-261. https://doi.org/10.1038/266259a0

78. Rossomando, E.F., and Sussman, M. (1973). A 5'-Adenosine monophosphate-dependent adenylate cyclase and an adenosine 3':5'-cyelic monophosphate-dependent adenosine triphosphate pyrophosphohydrolase in *Dictyostelium discoideum*. *Proc. Natl. Acad. Sci. USA* **70**, 1254-1257. https://doi.org/10.1073/pnas.70.4.1254

79. Rossomando, E.F., and Hesla, M.A. (1976). Time-dependent changes in *Dictyostelium discoideum* adenylate cyclase activity upon incubation with ATP. *J. Biol. Chem*. **251**, 6568-6573.

80. Saito, T., Taylor, G.W., Yang, J.C., Neuhaus, D., Stetsenko, D., Kato, A., and Kay, R.R. (2006). Identification of new differentiation inducing factors from *Dictyostelium discoideum*. *Biochimica. et Biophysica. Acta.* **1760**, 754-761. https://doi.org/10.1016/j.bbagen.2005.12.006

81. Saran, S., Azhar, M., Manogaran, P.S., Pande, G., and Nanjundiah, V. (1994). The level of sequestered calcium in vegetative amoebae of *Dictyostelium discoideum* can predict post-aggregative cell fate. *Differentiation* **57**, 163-169. https://doi.org/10.1046/j.1432-0436.1994.5730163.x

82. Sato, Y.G., Kagami, H.N., Narita, T.B., Fukuzawa, M., and Saito, T. (2013). Steely enzymes are involved in prestalk and prespore pattern formation. *Biosci. Biotech. Biochem*. **77**, 2008-2012. https://doi.org/10.1271/bbb.130294

83. Schell, J.C., Wisidagama, D.R., Bensard, C., Zhao, H., Wei, P., Tanner, J., Flores, A., Mohlman, J., Sorensen, L.K., Earl, C.S., Olson, K.A., Miao, R., Waller, T.C., Delker, D., Kanth, P., Jiang, L., DeBerardinis, R.J., Bronner, M.P., Li, D.Y., Cox, J.E., Christofk, H.R., Lowry, W.E., Thummel, C.S., and Rutter, J. (2017). Control of intestinal stem cell function and proliferation by mitochondrial pyruvate metabolism. *Nat. Cell Biol.* **19**, 1027-1036. https://doi.org/10.1038/ncb3593

84. Schindelin, J., Arganda-Carreras, I., Frise, E., Kaynig, V., Longair, M., Pietzsch, T., Preibisch, S., Rueden, C., Saalfeld, S., Schmid, B., Tinevez, J.Y., White, D.J., Hartenstein, V., Eliceiri, K., Tomancak, P., and Cardona, A. (2012). Fiji: an open-

source platform for biological-image analysis. *Nature Methods* **9**, 676-682. https://doi.org/10.1038/nmeth.2019.

85. Shadel, G.S., and Horvath, T.L. (2015). Mitochondrial ROS signaling in organismal homeostasis. *Cell* **163**, 560-569. https://doi.org/10.1016/j.cell.2015.10.001

86. Sherr, C.J. (1996). Cencer cell cycles. *Science* **274**, 1672-1677. https://doi.org/10.1126/science.274.5293.1672

87. Shiraki, N., Shiraki, Y., Tsuyama, T., Obata, F., Miura, M., Nagae, G., Aburatani, H., Kume, K., Endo, F., and Kume, S. (2014). Methionine metabolism regulates maintenance and differentiation of human pluripotent stem cells. *Cell Metab*. **19**, 780-794. https://doi.org/10.1016/j.cmet.2014.03.017

88. Sholl-Franco, A., Fragel-Madeira, L., Macama, A.C., Linden, R., and Ventura, A.L. (2010). ATP controls cell cycle and induces proliferation in the mouse developing retina. *Int. J. Dev. Neurosci*. **28**, 63-73. https://doi.org/10.1016/j.ijdevneu.2009.09.004

89. Simsek, T., Kocabas, F., Zheng, J., Deberardinis, R.J., Mahmoud, A.I., Olson, E.N., Schneider, J.W., Zhang, C.C., and Sadek, H.A. (2010). The distinct metabolic profile of hematopoietic stem cells reflects their location in a hypoxic niche. *Cell Stem Cell* **7**, 380–390. https:/doi.org/10.1016/j.stem.2010.07.011

90. Skog, S., Tribukait, B., and Sundius, G. (1982). Energy metabolism and ATP turnover time during the cell cycle of Ehrlich ascites tumour cells. *Exp. Cell Res.* **141**, 23-29. https://doi.org/10.1016/0014-4827(82)90063-5

91. Soboloff, J., Rothberg, B.S., Madesh, M., and Gill, D.L. (2012). STIM proteins: dynamic calcium signal transducers. *Nat. Rev. Mol. Cell Biol*. **13**, 549-565. https://doi.org/10.1038/nrm3414

92. Stefani, D.D., Raffaello, A., Teardo, E., Szabo, I., and Rizzuto, R. (2011). A forty-kilodalton protein of the inner membrane is the mitochondrial calcium uniporter. *Nature* **476**, 336-340. https://doi.org/10.1038/nature10230

93. Takubo, K., Nagamatsu, G., Kobayashi, C.I., Nakamura-Ishizu, A., Kobayashi, H.,

Ikeda, E., Goda, N., Rahimi, Y., Johnson, R.S., Soga, T., Hirao, A., Suematsu, M., and Suda, T. (2013). Regulation of glycolysis by Pdk functions as a metabolic checkpoint for cell cycle quiescence in hematopoietic stem cells. *Cell Stem Cell* **12**, 49-61. https://doi.org/10.1016/j.stem.2012.10.011

94. Tan, B.S.N., Lonic, A., Morris, M.B., Rathjen, P.D., and Rathjen, J. (2011). The amino acid transporter SNAT2 mediates L-proline-induced differentiation of ES cells. *Am. J. Physiol. Cell Physiol.* **300**, C1270-1279. https://doi.org/10.1152/ajpcell.00235.2010

95. Tanaka, Y., Itakura, R., Amagai, A., and Maeda, Y. (1998). The signals for starvation response are transduced through elevated $[Ca^{2+}]^i$ in *Dictyostelium* cells. *Exp. Cell Res.* **240**, 340–348. https://doi.org/10.1006/excr.1998.3947

96. Tasaka, M., and Takeuchi, I. (1981). Role of cell sorting in pattern formation in *Dictyostelium discoideum*. *Differentiation* **18**, 191-196. https://doi.org/10.1111/j.1432-0436.1981.tb01122.x

97. Thompson, C.R.L., and Kay, R.R. (2000). Cell-fate choice in *Dictyostelium*: intrinsic biases modulate sensitivity to DIF signaling. *Dev. Biol*. **227**, 56-64. https://doi.org/10.1006/dbio.2000.9877

98. Traynor, D., Kessin, R.H., and Williams, J.G. (1992). Chemotactic sorting to cAMP in the multicellular stages of *Dictyostelium* development. *Proc. Natl. Acad. Sci. USA* **89**, 8303-8307. https://doi.org/10.1073/pnas.89.17.8303

99. Tsuyama, T., Kishikawa, J., Han, Y.W., Harada, Y., Tsubouchi, A., Noji, H., Kakizuka, A., Yokoyama, K., Uemura, T., and Imamura, H. (2013). In vivo fluorescent adenosine 5'-triphosphate (ATP) imaging of *Drosophila melanogaster* and *Caenorhabditis elegans* by using a genetically encoded fluorescent ATP biosensor optimized for low temperatures. *Anal. Chem.* **85**, 7889-7896. https://doi.org/10.1021/ac4015325

100. Veltman, D.M., Akar, G., Bosgraaf, L., and Van Haastert, P.J. (2009). A new set of small, extrachromosomal expression vectors for *Dictyostelium discoideum*. *Plasmid* **61**, 110-118. https://doi.org/10.1016/j.plasmid.2008.11.003

101. Weijer, C.J., Duschi, G., and David, C.N. (1984). A revision of the *Dictyostelium discoideum* cell cycle. *J. Cell Sci*. **70**, 111-131.

102. Williams, J.G. (2010). *Dictyostelium* finds new roles to model. *Genetics* **185**, 717-726. https://doi.org/10.1534/genetics.110.119297

103. Yang, P., Shen, W.B., Reece, E.A., Chen, X., and Yang, P. (2016). High glucose suppresses embryonic stem cell differentiation into neural lineage cells. *Biochem. Biophys. Res. Commun.* **472**, 306-312. https://doi.org/10.1016/j.bbrc.2016.02.117

104. Zada-Hames, I.M., and Ashworth, J.M. (1978). The cell cycle and its relationship to development in *Dictyostelium discoideum*. *Dev. Biol.* **63**, 307-320. https://doi.org/ 10.1016/0012-1606(78)90136-7

105. Zakrzewski, W., Dobrzynski, M., Szymonowicz, M., and Rybak, Z. (2019). Stem cells: past, present, and future. *Stem Cell Res. Ther.* **10**, 68. https://doi.org/ 10.1186/s13287-019-1165-5

106. Zimmerman, J.J., Andre-von Arnim, A.S., and McLaughlin, J. (2011). *Cellular Respiration. In Pediatric Critical Care, 4th edition.* pp.1058-1072, https://doi.org/10. 1016/B978-0-323-07307-3.10074-6

8. Acknowledgement

First of all, I really appreciate to all members of Hiraoka laboratory for their kind helps. I want to thank them for teaching me the fun of discussion. Especially, Professor Yasushi Hiraoka and Tokuko Haraguchi gave me a lot of suggestion and comments in proceeding this research. This research could achieve nothing without their help. I really thank for helping me. Dr. Yasuhiro Hirano also gave me helpful suggestion about the methods of fluorescence microscopic observation and analysis of their results. Dr. Tadashi Nakano thankfully considered the analysis methods of cell tracking and gave me suggestion. Miss Chie Mori made a lot of plasmid constructions for me. Dr. Takeshi Sakuno, Dr. Yoko Hayashi, Dr. Hidesato Ogawa, and Dr. Haruhiko Asakawa often gave me comments for improvement of this research. I want to express my sincere thanks to them again.

Dr. Satoshi Kuwana and Professor Masashi Fukuzawa provided me the really important experimental system. Thanks for discussing with me and giving me a lot of kind helps. Although it was short period, I was really pleased to stay at his laboratory as internship. The experiences obtained there is my best treasure. I also appreciate to Mr. Narufumi Kameya and Mr. Kenichi Abe as they often discussed with me and informed the interesting results and papers.

Dr. Yukihiro Miyanaga, Mr. Shinichi Yamazaki, Mr. Takuma Degawa, Dr. Yuki Tanabe, and Dr. Hidenori Hashimura, members in Ueda laboratory of Osaka university, gave me various plasmid constructs and *Dictyostelium* cell strains. Especially, Mr. Degawa, Dr. Tanabe, and Dr. Hashimura also gave me a lot of suggestion and comments. Mr. Yamazaki, Mr. Daisuke Yoshioka, Dr. Kaori Tanabe, Dr. Yoichiro Kamimura, and Professor Masahiro Ueda provided me experimental environment to support this research.

Finally, I want to express my sincere thanks to my family and friends supporting my daily life. I appreciate to my family, especially my parents, for providing me the environment to drive to the long-time research without any concerns. Also, The time spent with my friends always gave me relaxing and enjoyable time; it allowed me drive to the writing of this thesis. Thanks to the many precious friends who always supported me in my hard times, especially to HM, YF, and YI.

9. Achievement list

【 原著論文 】

1. Intracellular ATP levels influence cell fates in *Dictyostelium discoideum* differentiation. (2020 年 3 月) "*Genes to Cells*" (*in press*), https://doi.org/10.1111/gtc.12763
   ［著者］Haruka Hiraoka, Tadashi Nakano, Satoshi Kuwana, Masashi Fukuzawa, Yasuhiro Hirano, Masahiro Ueda, Tokuko Haraguchi, Yasushi Hiraoka

【 収録論文 】

1. Cellular and chromosomal alterations in response to acentric chromosome formation (2019 年 8 月)
   The 7th International Symposium on Frontier Technology in Pattaya, Thailand (Paper ID 40)
   ［著者］Haruka Hiraoka, Keisuke Morita, Yuko Ohno, Riku Kuse, Yuki Ogiyama, Yoshino Kubota, Fumio Matsuda, Hiroshi Shimizu, Kojiro Ishii

【 国際会議 】

1. Small cell aggregation method which enables us to observe all cell's behavior individually (ポスター)
   Biophysical Society 59th Annual Meeting (Baltimore, Maryland, US / 2015 年 2 月)
   ［発表者］○Haruka Hiraoka, Masahiro Ueda
2. Cellular and chromosomal alterations in response to acentric chromosome formation (口頭発表)
   ***収録論文 1**
   The 7th International Symposium on Frontier Technology (Pattaya, Thailand / 2019 年 8 月)
   ［発表者］○Haruka Hiraoka, Keisuke Morita, Yuko Ohno, Riku Kuse, Yuki Ogiyama, Yoshino Kubota, Fumio Matsuda, Hiroshi Shimizu, Kojiro Ishii

【 国内の学会・研究会 】

口頭発表

1. 細胞性粘菌における PEPC を介した分化制御　　***優秀発表賞 受賞**
   第 8 回 東北植物学会 (弘前大学 文京町地区キャンパス / 2018 年 12 月)
   ［発表者］○亀谷匠郁, 平岡陽花, 桑名悟史, 田岡和晃, 福澤雅志
2. ATP-dependent cell fate determination in *Dictyostelium discoideum*
   第 5 回 細胞生物若手の会 蛋白質科学若手研究者 合同交流会 (三宮研修センター / 2019 年 6 月)
   ［発表者］○平岡陽花, 桑名悟史, 福澤雅志, 上田昌宏, 原口徳子, 平岡泰
3. ATP-dependent cell fate determination in *Dictyostelium discoideum*　　***一般演題から採択**
   第 71 回 日本細胞生物学会 (神戸国際会議場 / 2019 年 6 月)
   シンポジウム「時間と場による発生制御のメカニズム」(オーガナイザー：川口大地、川口喬吾)
   ［発表者］○平岡陽花, 桑名悟史, 福澤雅志, 上田昌宏, 原口徳子, 平岡泰
4. 分化運命決定における ATP 依存性　　***ベストプレゼン賞 受賞**
   第 9 回 日本細胞性粘菌学会 (順天堂大学 さくらキャンパス / 2019 年 10 月)
   ［発表者］○平岡陽花, 桑名悟史, 福澤雅志, 上田昌宏, 原口徳子, 平岡泰

ポスター発表

1. 集合体中の位置に応じた遺伝子発現解析
   第 5 回 日本細胞性粘菌学会 (弘前大学 文京町地区キャンパス / 2015 年 10 月)
   ［発表者］○平岡陽花, 上田昌宏

2. 低グルコース環境下での培養がもたらす発生進行の遅延
   第 6 回 日本細胞性粘菌学会 (上智大学 / 2016 年 10 月)
   ［発表者］○平岡陽花, 上田昌宏
3. Prestalk cell subtype pstVA の増殖期における遺伝子発現パターン
   第 7 回 日本細胞性粘菌学会 (立命館大学 びわこ・くさつキャンパス / 2017 年 10 月)
   ［発表者］○平岡陽花, 桑名悟史, 福澤雅志, 上田昌宏
4. Prestalk cell subtype pstVA の増殖期における細胞特性 ***ベストプレゼン賞 受賞**
   第 8 回 日本細胞性粘菌学会 (山口大学 吉田キャンパス / 2018 年 10 月)
   ［発表者］○平岡陽花, 桑名悟史, 福澤雅志, 上田昌宏
5. ATP-dependent cell fate determination in *Dictyostelium discoideum*
   クロマチン潜在能 第 2 回領域会議 (ホテル竹島 / 2019 年 6 月)
   ［発表者］○Haruka Hiraoka, Sathoshi Kuwana, Masashi Fukuzawa, Masahiro Ueda, Tokuko Haraguchi, Yasushi Hiraoka
6. ATP-dependent cell fate determination in *Dictyostelium discoideum*
   第 71 回 日本細胞生物学会 (神戸国際展示場 / 2019 年 6 月)
   ［発表者］○Haruka Hiraoka, Sathoshi Kuwana, Masashi Fukuzawa, Masahiro Ueda, Tokuko Haraguchi, Yasushi Hiraoka
7. ATP-dependent cell fate determination in *Dictyostelium discoideum*
   第 11 回 光塾 (理化学研究所 神戸キャンパス / 2019 年 11 月 12-13 日予定, 登録済み)
   ［発表者］○Haruka Hiraoka, Sathoshi Kuwana, Masashi Fukuzawa, Masahiro Ueda, Tokuko Haraguchi, Yasushi Hiraoka

【 大阪大学・理研 (学内・所内イベント) での発表 】

1. 細胞集合の中心を決めるメカニズムについて (口頭発表) ***優秀発表賞 受賞**
   大阪大学 理学部 生物科学科 生命理学コース 卒業研究発表会 (2014 年 2 月)
   ［発表者］○平岡陽花, 上田昌宏
2. Determination of cell aggregation center and small aggregation system (ポスター)
   The 8th Young Researcher's Retreat (KKR 京都くに荘 / 2014 年 7 月)
   ［発表者］○Haruka Hiraoka, Masahiro Ueda
3. The difference of developmental stage corresponding to the cell position (ポスター)
   QBiC Retreat 2015 (RIKEN Quantitative Biology Center / 2015 年 6 月)
   ［発表者］○Haruka Hiraoka, Masahiro Ueda
4. 発生分化初期の多細胞体における遺伝子発現解析 (口頭発表)
   大阪大学大学院 生命機能研究科 生命機能専攻 修士論文公聴会 (2016 年 2 月)
   ［発表者］○平岡陽花, 上田昌宏
5. The difference of cell state in the formation of aggregates (ポスター)
   QBiC Retreat 2016 (淡路夢舞台国際会議場 / 2016 年 6 月)
   ［発表者］○Haruka Hiraoka, Masahiro Ueda
6. The difference of cell state in the formation of aggregates (ポスター)
   The 10th Young Researcher's Retreat (KKR 京都くに荘 / 2016 年 7 月)
   ［発表者］○Haruka Hiraoka, Masahiro Ueda
7. The reveal of mechanism to sense each other cell's conditions among cell population (ポスター)
   Humanware International Symposium 2017 (Senri Hankyu Hotel, Osaka, Japan / 2017 年 1 月)
   ［発表者］○Haruka Hiraoka, Masahiro Ueda
8. 細胞性粘菌の分化運命は細胞内 ATP 濃度に依存する (ポスター) ***ベストプレゼン賞 受賞**
   大阪大学大学院 生命機能研究科リトリート交流会 (淡路夢舞台国際会議場 / 2019 年 5 月)
   ［発表者］○平岡陽花, 桑名悟史, 福澤雅志, 上田昌宏, 原口徳子, 平岡泰